

Article

Characteristics and Genetic Mechanism of Pore Throat Structure of Shale Oil Reservoir in Saline Lake—A Case Study of Shale Oil of the Lucaogou Formation in Jimsar Sag, Junggar Basin

Xiaojun Zha ^{1,2}, Fuqiang Lai ^{1,2,*}, Xuanbo Gao ^{1,2,*} , Yang Gao ³, Nan Jiang ^{1,2}, Long Luo ^{1,2}, Yingyan Li ³, Jia Wang ^{1,2}, Shouchang Peng ³, Xun Luo ^{1,2} and Xianfeng Tan ^{1,2,*}

¹ College of Petroleum and Gas Engineering, Chongqing University of Science and Technology, Chongqing 401331, China; zzzzzz662021@163.com (X.Z.); nanjiang@cqust.edu.cn (N.J.); longluo988@163.com (L.L.); wangjia@cqust.edu.cn (J.W.); luoxununn@163.com (X.L.)

² Chongqing Key Laboratory of Complex Oil and Gas Exploration and Development, Chongqing 401331, China

³ Research Institute of Exploration and Development, PetroChina Xinjiang Oilfield Company, Kelamayi 834000, China; gao-yang@petrochina.com.cn (Y.G.); fdyy@petrochina.com.cn (Y.L.); psc@petrochina.com.cn (S.P.)

* Correspondence: laifq1982@163.com (F.L.); gaouxuanbo@cqust.edu.cn (X.G.); xianfengtan8299@163.com (X.T.)



Citation: Zha, X.; Lai, F.; Gao, X.; Gao, Y.; Jiang, N.; Luo, L.; Li, Y.; Wang, J.; Peng, S.; Luo, X.; et al. Characteristics and Genetic Mechanism of Pore Throat Structure of Shale Oil Reservoir in Saline Lake—A Case Study of Shale Oil of the Lucaogou Formation in Jimsar Sag, Junggar Basin. *Energies* **2021**, *14*, 8450. <https://doi.org/10.3390/en14248450>

Academic Editors: Xixin Wang, Luxing Dou and Yuming Liu

Received: 18 November 2021

Accepted: 11 December 2021

Published: 14 December 2021

Publisher's Note: MDPI stays neutral with regard to jurisdictional claims in published maps and institutional affiliations.



Copyright: © 2021 by the authors. Licensee MDPI, Basel, Switzerland. This article is an open access article distributed under the terms and conditions of the Creative Commons Attribution (CC BY) license (<https://creativecommons.org/licenses/by/4.0/>).

Abstract: The shale oil reservoir of the Lucaogou Formation in the Jimsar Sag has undergone tectonic movement, regional deposition and complex diagenesis processes. Therefore, various reservoir space types and complex combination patterns of pores have developed, resulting in an intricate pore throat structure. The complex pore throat structure brings great challenges to the classification and evaluation of reservoirs and the efficient development of shale oil. The methods of scanning electron microscopy, high-pressure mercury injection, low-temperature adsorption experiments and thin-slice analysis were used in this study. Mineral, petrology, pore throat structure and evolution process characteristics of the shale oil reservoir were analyzed and discussed qualitatively and quantitatively. Based on these studies, the evolution characteristics and formation mechanisms of different pore throat structures were revealed, and four progressions were made. The reservoir space of the Lucaogou Formation is mainly composed of residual intergranular pores, dissolved pores, intercrystalline pores and fractures. Four types of pore throat structures in the shale oil reservoir of the Lucaogou Formation were quantitatively characterized. Furthermore, the primary pore throat structure was controlled by a sedimentary environment. The pores and throats were reduced and blocked by compaction and cementation, which deteriorates the physical properties of the reservoirs. However, the dissolution of early carbonate, feldspar and tuffaceous minerals and a small amount of carbonate cements by organic acids are the key factors to improve the pore throat structure of the reservoirs. The genetic evolution model of pore throat structures in the shale oil reservoir of the Lucaogou Formation are divided into two types. The large-pore medium-fine throat and medium-pore medium-throat reservoirs are mainly located in the delta front-shallow lake facies and are characterized by the diagenetic assemblage types of weak compaction–weak carbonate cementation–strong dissolution, early medium compaction–medium calcite and dolomite cementation–weak dissolution. The medium-pore fine throats and fine-pore fine throats are mainly developed in shallow lakes and semi-deep lakes. They are characterized by the diagenetic assemblage type of strong compaction–strong calcite cementation–weak dissolution diagenesis. This study provides a comprehensive understanding of the pore throat structure and the genetic mechanism of a complex shale oil reservoir and benefits the exploration and development of shale oil.

Keywords: Jimsar Sag; Lucaogou Formation; shale oil reservoir; pore throat structure; genetic mechanism

1. Introduction

In recent years, the exploration and development of shale oil have developed rapidly in China, which is currently a research hotspot of unconventional hydrocarbon resources [1–4].

In China, shale oil is mainly developed in Mesozoic and Cenozoic lacustrine shale strata in the continental basins. It has huge exploration and development potential [5–9]. Compared with other reservoirs, shale oil reservoirs are usually characterized by a combination of multi-scale, multi-type pores, fractures and pore throat structures [10–13]. The study of microscopic scale pore structure is very important for unconventional reservoir evaluation [14,15], especially for shale oil reservoirs with complex sedimentary environments, rapid lithological changes and strong heterogeneity. It is difficult to identify the type of microscopic pore throat structure due to the significant variation of the size of the nano-scale pore throat. The complex pore throat structure has also brought great challenges to the quantitative characterization of the pore throat structure in shale oil reservoirs, which seriously hinders the comprehensive evaluation and efficient exploration of shale oil [16–21]. Many scholars have proposed discriminant indexes for pore throat structure and realized a quantitative characterization of pore throat structure. For example, Liu Li et al. used the high-pressure mercury intrusion testing technology to obtain the microscopic pore structure parameters of pore throat size, distribution and connectivity of shale oil reservoirs in the Jiyang Depression and analyzed the contribution degree of different scale pore throats to seepage capacity. The previous researches mainly focused on a single layer and discussed the characterization techniques of the pore throat structure of different lithologies in shale oil reservoirs [22–27]. These studies deepen the understanding of the pore throat structure in shale oil reservoirs. However, the microstructure and genetic mechanism between layers have not been compared, and the effects of sedimentation and diagenetic evolution on microscopic pore throat structure have not been explained.

The shale oil in Jimsar Sag, Junggar Basin, is the first national shale oil demonstration area in China. It has been a hot spot in the field of shale oil exploration and development [10]. The depositional environment of the reservoir of the Lucaogou Formation in Jimsar Sag is in a typical salty lacustrine, which is characterized by different types of lithologies. The Lucaogou Formation has experienced complex deposition, diagenesis and transformation due to the alternation action between tectonic movement and acid-base fluids. Therefore, the shale oil reservoir in Jimsar Sag shows a complex pore throat structure and obvious heterogeneity [28,29]. At present, some problems about the studies of the shale oil reservoir in Jimsar Sag to be resolved are: (1) the methods of quantitative characterization and classification of the pore structure in the shale oil reservoir are not established; (2) the primary controlling factors of the difference of the pore structure in the shale oil reservoir are not revealed. (3) The genetic evolution models of different pore throat structures are still unclear. Therefore, solving these problems has great significance in improving the exploration and development of shale oil.

In this study, the mineral, petrology, pore throat structure and evolution process characteristics of shale oil reservoir were discussed qualitatively and quantitatively by the methods of scanning electron microscopy, high-pressure mercury injection, low-temperature adsorption experiments and thin-slice analysis. We finally established the genetic evolution model of the pore throat structure in the shale oil reservoir. This study clarifies the pore throat structure and the genetic mechanism of a complex lithological shale oil reservoir and benefits the exploration and development of shale oil.

2. Geological Setting

The Jimsar Sag is located southwest of the eastern uplift of the Junggar Basin (Figure 1a). It is deposited on the folded basement of Middle Carboniferous with obvious boundary characteristics [30–32]. The depression is bounded by the Xidi Fault and Qing1 Well South 1 fault to the west, the Jimsar Fault to the north, and the Santai Fault to the south (Figure 1b).

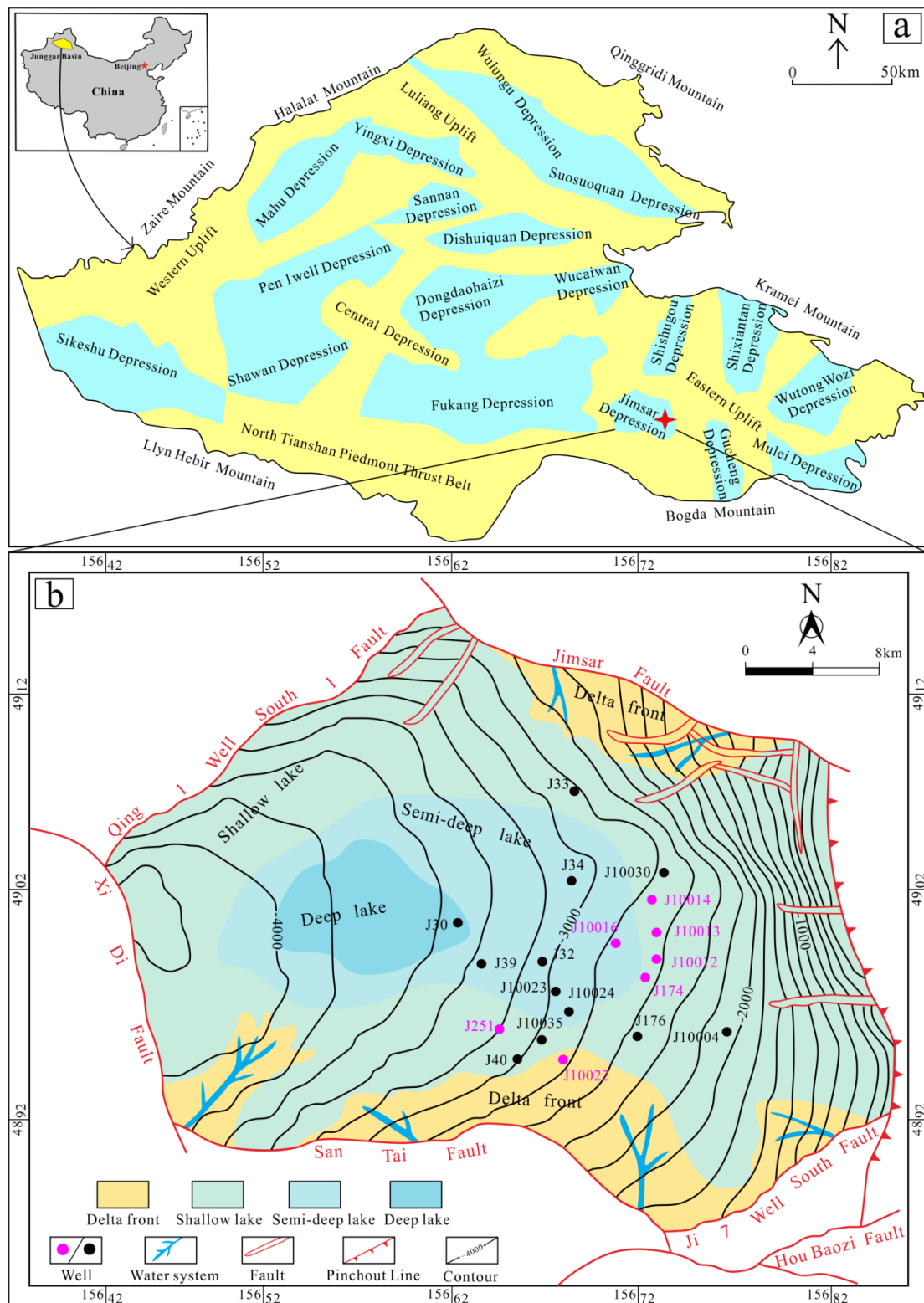


Figure 1. Geographical location (a) and regional structural map (b) of Jimsar Sag in the Junggar Basin.

The Jimsar Sag has experienced multiple tectonic movements such as Hercynian, Indo-China, Yanshan and Himalayas [33]. These tectonic movements made the west subside and the east uplift. Faulting and uplifting occurred simultaneously in the south and north, but the intensity of deformation was higher in the north. All formations below the Cretaceous in the eastern part suffered denudation. In general, the Lucaogou Formation deposited

a relatively complete set of strata from the Permian to the Quaternary [34–37] (Figure 2). The Lucaogou Formation is thick in the west and south, and becomes thin towards the surrounding uplifts (Figure 3).

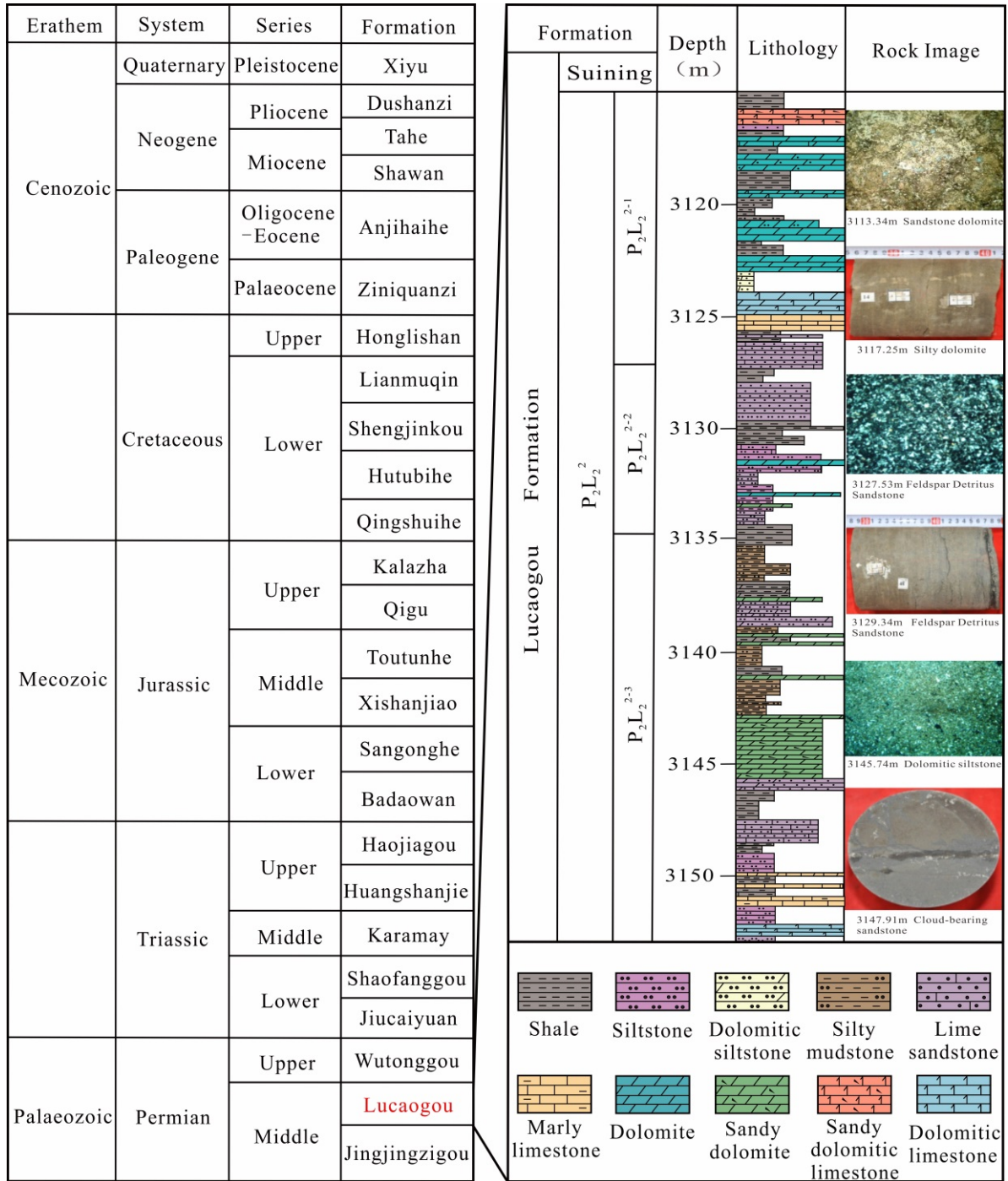


Figure 2. Stratigraphic column of Jimsar Sag in the Junggar Basin.

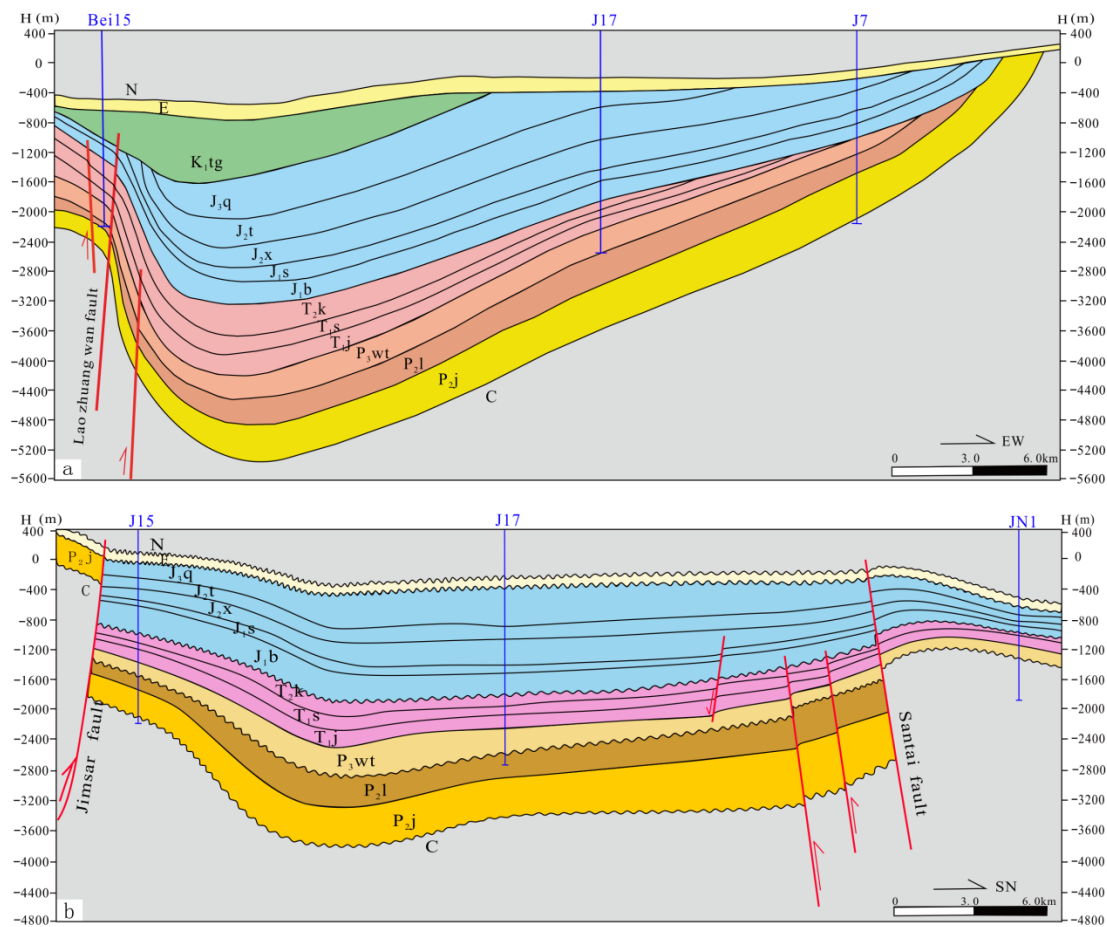


Figure 3. E-W (a) and S-N Stratigraphic characteristics (b) of Jimsar Sag in Junggar Basin.

During the deposition period of the Lucaogou Formation, the provenance mainly came from the surrounding paleo-uplift. The climate was arid and the salinity of water was high, which were beneficial for the accumulation of organic matter and the chemical precipitation of dolomite. With the continual increase in water salinity, a large number of alkaline minerals were developed in the sag and a relatively independent saline lacustrine deposition system was formed [34].

3. Data and Methods

This study was based on geological data from six wells covering the different sedimentary facies. The X-ray diffraction (XRD) analysis, physical property analysis and scanning electron microscopy (SEM) were used to determine the reservoir characteristics of the Lucaogou Formation in Jimsar Sag. Then, the pore throat structure was described quantitatively by the CT scan, nitrogen adsorption experiment and high-pressure mercury intrusion experiment. The genetic evolution model will be established by the diagenetic evolution sequence and different diagenesis.

4. Results

4.1. Petrological and Mineralogical Characteristics

The shale oil reservoir of the Lucaogou Formation in the Jimsar Sag has complex lithology. The dominant lithology of the Lucaogou Formation can be divided into two categories and six subcategories under the microscope (Figure 4). Clastic rocks are mainly fine-grained sediments, including the dolomite sandstone, fine dolomite sandstone, lithic feldspar fine sandstone and silty mudstone. Carbonate rocks are mainly microcrystalline dolomite and sandy dolomite.

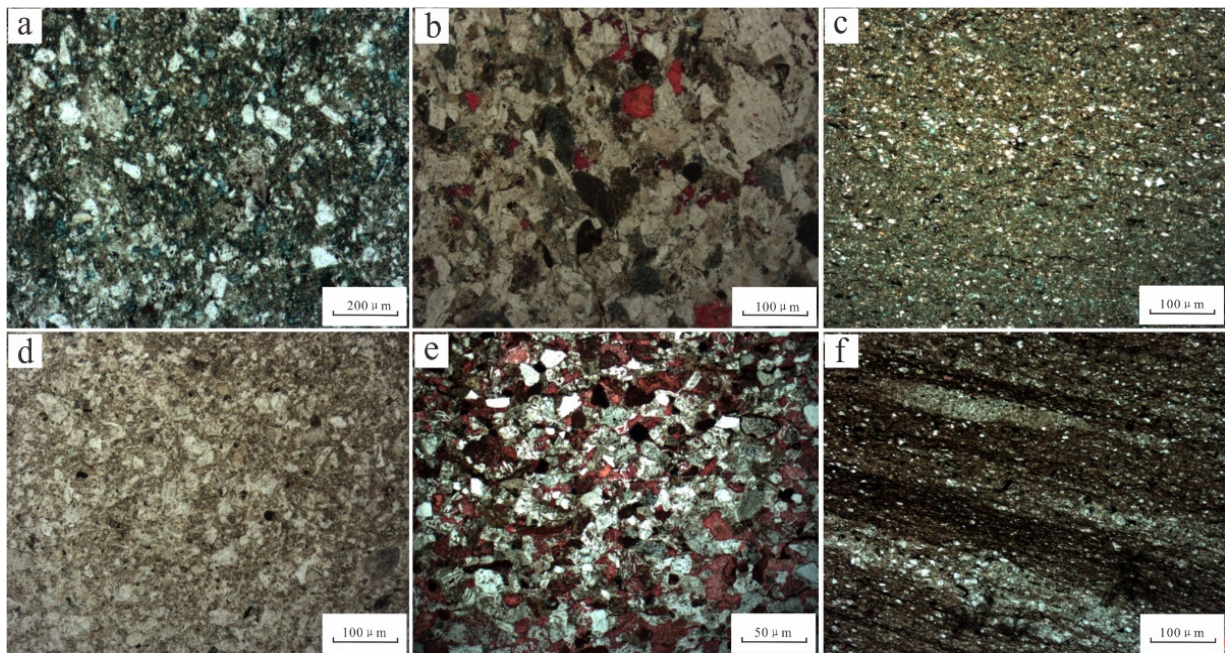


Figure 4. Rock types of the Lucaogou Formation in Jimsar Sag. (a). Sandy dolomite. J10012, 3171.7 m, $(-)\times 200$. Dolomite minerals and felsic minerals are the main mineral compositions and the intergranular pores are filled with organic matter; (b). Dolomite sandstone. J10016, 3456.37 m, $(-)\times 100$. The intergranular dissolution pores are filled with organic matter; (c). Dolomite siltstone, J10016, 3320.82 m, $(-)\times 100$. The dolomite minerals in the form of microscopic particles are the main mineral compositions. The intergranular pores (slits) are distributed along the layer and filled with organic matter; (d). Microcrystalline dolomite. J10012, 3195.73 m, $(-)\times 100$. The dolomite minerals and felsic minerals are the main mineral compositions, the intergranular micropores are filled with organic matter; (e). Feldspar detritus sandstone. J10014, 3233.38 m, $(-)\times 50$. The pores are mainly the residual intergranular pores with fine-grained sand-like structure, and the pores are filled with some of the organic matter; (f). Silty mudstone, J10013, 3192.55 m, $(-)\times 100$. Some of the silt sand developed in the horizontal bedding.

The mineral components of the Lucaogou Formation in Jimsar Sag mainly consist of carbonate components, terrigenous clastic components and pyroclastic components. The minerals mainly consist of quartz, potash feldspar, plagioclase, calcite, dolomite, iron dolomite, clay minerals and other minerals (Figure 5). The average of feldspar mainly varies from 5.8% to 29.3%, including potash feldspar and plagioclase. The averages of quartz and dolomite are similar. The average content of clay is relatively low with an average of 8.6%. Frequent changes in the vertical distribution indicate that the rock types of the Lucaogou Formation in Jimsar Sag are complex and changeable (Figure 6). The frequent changes also reflect that the shale oil reservoir of the Lucaogou Formation in the Jimsar Sag develops a set of mixed sedimentary rocks.

4.2. Physical Characteristics

The core porosity varies from 0.49 to 21.80% and is mainly distributed in 6.0–19.0% with an average of 11.35%. The core permeability varies from 0.01 to 1.24 mD and mainly distributed in 0.01–0.10 mD with an average of 0.14 mD (Table 1). The correlation between the porosity and permeability of the Lucaogou Formation shale oil reservoir in the Jimsar Sag is poor. The range of permeability corresponding to the same porosity varies greatly, reflecting the complex porosity–permeability relationship of the shale oil reservoir in the Lucaogou Formation of Jimsar Sag (Figure 7).

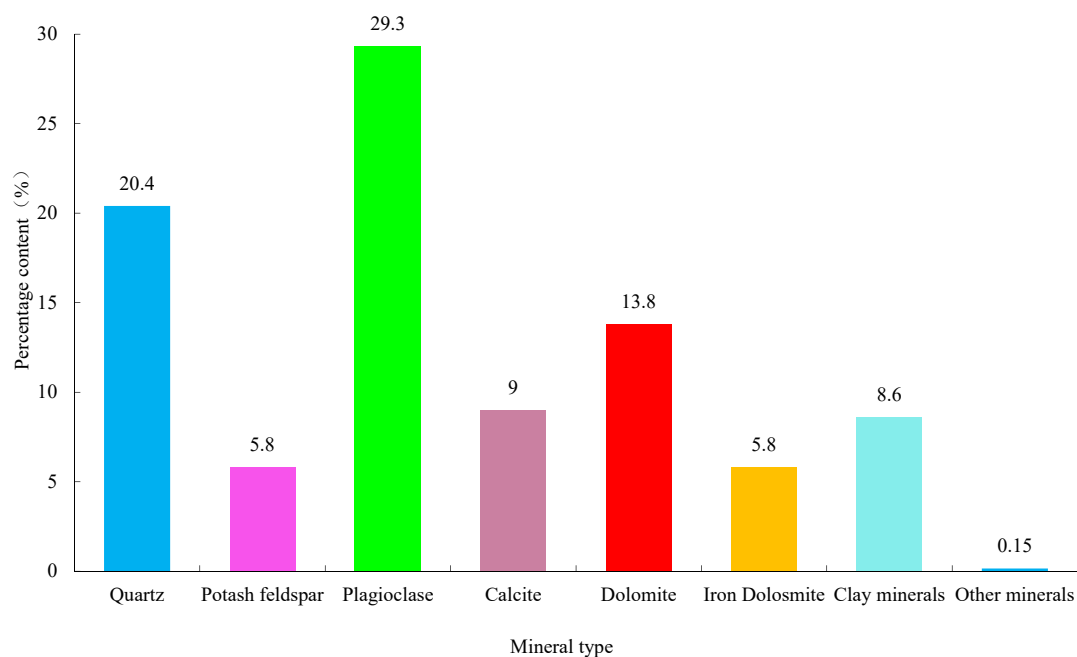


Figure 5. Mineral types of the Lucaogou Formation in Jimsar Sag.

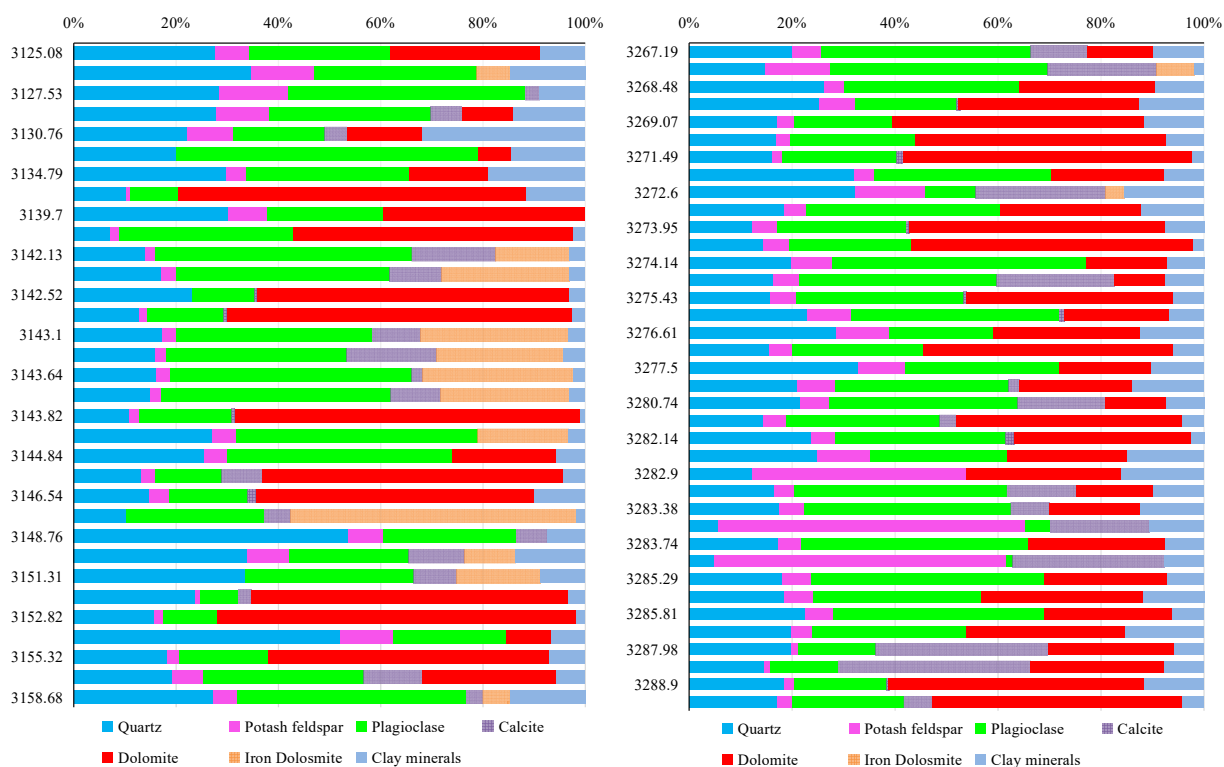


Figure 6. Mineralogical characteristics of the Lucaogou Formation in the Jimsar Sag.

Table 1. Porosity and permeability of the reservoir.

| Physical Parameters | Minimum | Max | Main Interval | Average |
|---------------------|---------|-------|---------------|---------|
| Porosity/% | 0.49 | 21.80 | 6.0–19.0 | 11.35 |
| Permeability/mD | 0.01 | 1.24 | 0.01–0.10 | 0.14 |

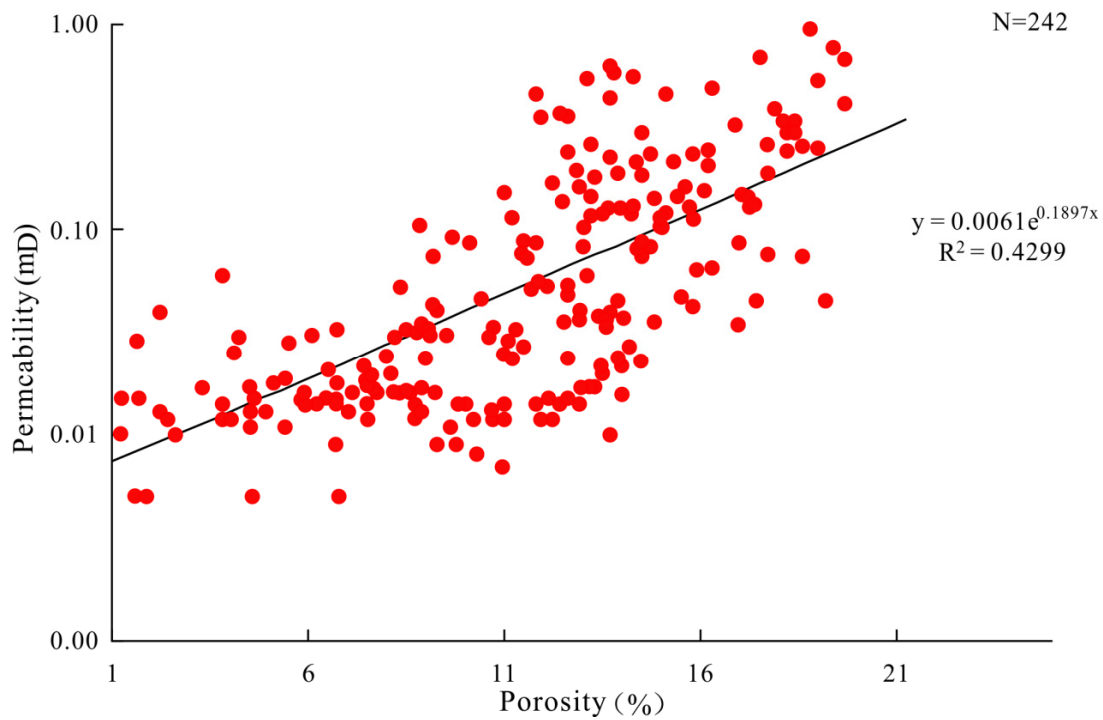


Figure 7. Correlation diagram of the porosity and permeability of the Lucaogou Formation.

The physical properties of different lithologies are quite different (Figures 8 and 9). The porosity of feldspar detritus sandstone mainly ranges from 6.0 to 10.0% and the permeability is mainly distributed in 0.01–1.00 mD. The porosity of dolomitic sandstone mainly ranges from 2.0 to 8.0%, and the permeability is mainly distributed in 0.01–0.02 mD. The porosity of sandstone dolomite mainly ranges from 4.0 to 8.0%, and the permeability is mainly distributed in 0.01–0.32 mD (Table 2). In general, the feldspar detritus sandstone has the best physical properties and the sandy dolomite is relatively poor.

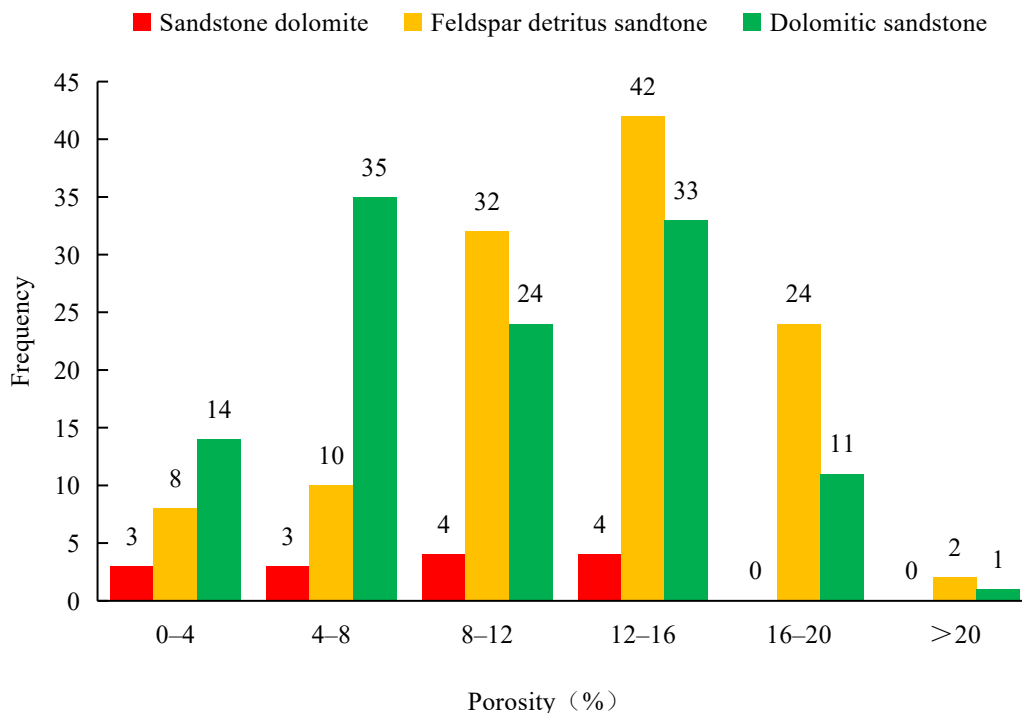


Figure 8. Frequency distribution of the porosity of the different lithologies in the Lucaogou Formation.

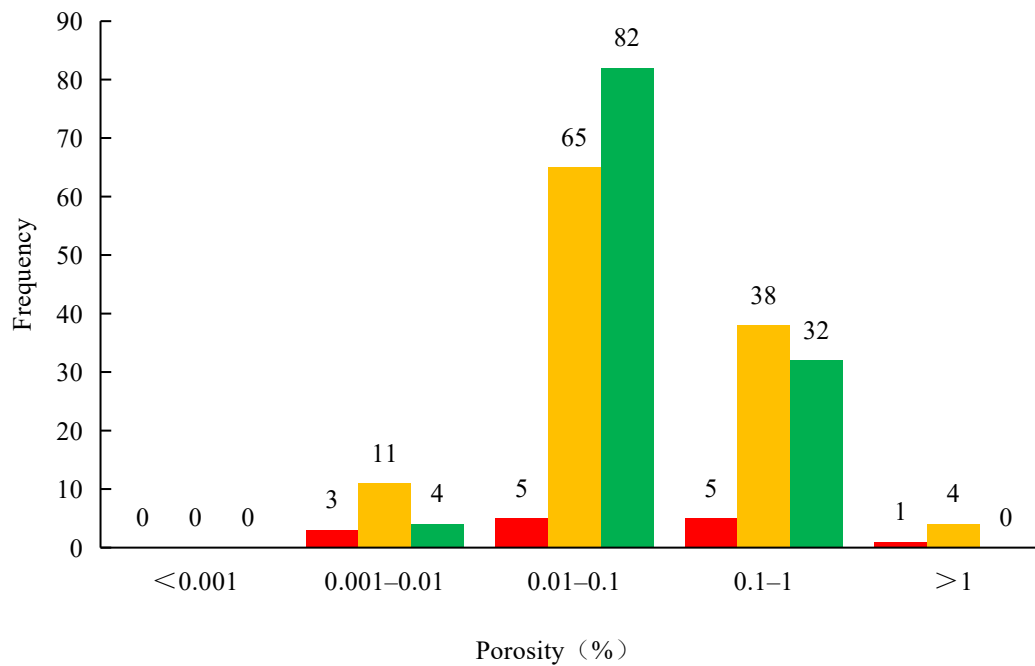


Figure 9. Frequency distribution of the permeability of the different lithologies in the Lucaogou Formation.

Table 2. Porosity and permeability of the various reservoir rocks.

| Physical Parameters | Lithology | | | |
|---------------------|-----------------------------|---------------------|----------------|-----------|
| | Feldspar Detritus Sandstone | Dolomitic Sandstone | Sandy Dolomite | |
| Porosity/% | Max | 21.80 | 13.80 | 19.80 |
| | Minimum | 0.50 | 0.49 | 1.58 |
| | Main interval | 6.0–10.0 | 2.0–8.0 | 4.0–8.0 |
| | Average | 11.97 | 9.98 | 8.54 |
| | Standard deviation | 4.52 | 4.88 | 4.65 |
| Permeability/mD | Max | 1.24 | 1.13 | 1.83 |
| | Minimum | 0.01 | 0.03 | 0.01 |
| | Main interval | 0.01–1.00 | 0.01–0.02 | 0.01–0.32 |
| | Average | 0.18 | 0.10 | 0.04 |
| | Standard deviation | 0.29 | 0.10 | 0.47 |

4.3. Diagenesis Characteristics

4.3.1. Compaction

The shale oil reservoir has widely experienced a medium-intense degree of compaction, which can be divided into chemical and mechanical types. The dolomite has a single component and a massive structure with relatively strong compaction. The massive felsic minerals in the sandy dolomite are distributed directionally by the compaction (Figure 10a). The content of quartz gradually increases, resulting in the increase in porosity and the reduction in compaction. The mineral particles in the dolomite siltstone are in obvious line contact. The sandy dolomite has medium compaction strength and poor rounding.

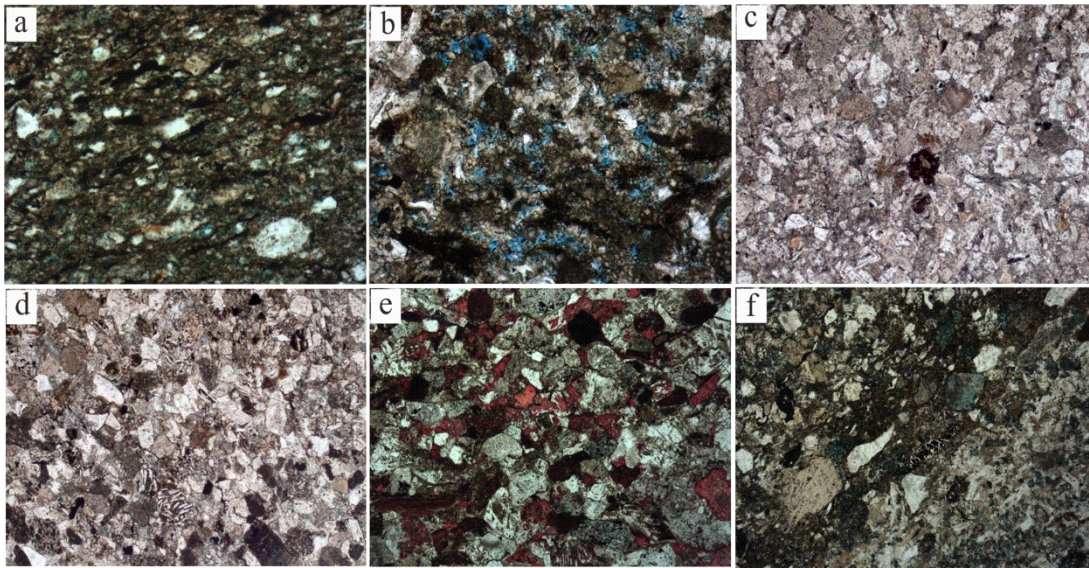


Figure 10. Diagenesis types of the Lucaogou Formation in Jimsar Sag. (a). Sandy dolomite, J10016, 3320.82 m, $(-)\times 200$. The silty felsic minerals show a directional distribution, and a small amount of iron dolomite crystals are uniformly distributed. Some intergranular micropores are filled with organic matter; (b). Feldspar detritus sandstone, J10012, 3157.7 m, $(-)\times 100$. The dissolved pores of feldspar are developed. Residual intergranular pores and intergranular dissolved pores are filled with some organic matter; (c). Lime sandstone, J251, 3767.61 m, $(-)\times 50$. The cementation is strong. The calcite has the fine-grained structure among the clastic particles, and the surface of the feldspar particles is dirty from dissolving soil; (d). Feldspar detritus sandstone, J43, 3495.83 m, $(-)\times 50$. The calcite is squeezed between clastic particles and produced in the form of cement. A large amount of andesite lithic sandstone and pyrite are filled in the intergranular pores; (e). Feldspar detritus sandstone. J10014, 3233.38 m, $(-)\times 50$. Fine-grained sand-like structure. The pores are mainly the residual intergranular pores and most of the organic matter is filled in the pores; (f). Feldspar detritus sandstone, J10012, 3157.7 m, $(-)\times 100$. Feldspar is dolomitized by iron dolomite. Intergranular dissolved pores are filled by dolomite and clay mixed base. The residual intergranular pores are filled with some organic matter.

4.3.2. Dissolution

The shale oil reservoir has an obvious dissolution phenomenon under the action of acid-base fluid alternating dissolution transformation. The physical properties of the reservoir have been greatly improved (Figure 10b,e). The surface or edge of quartz and feldspar mineral particles in sandy dolomite and lime dolomite has different degrees of dissolution. The intercrystalline pores of dolomite are relatively developed and filled with organic matter. The dissolution of dolomitic sandstone is relatively strong. The microcrystalline clay minerals, felsic minerals, and microscopic dolomite minerals are distributed alternately in the rock. The micropores between grains are directional and most of the pores are filled with organic matter.

4.3.3. Cementation

The shale oil reservoir has different types of cementation. It is mainly based on calcite cementation, clay mineral cementation and siliceous cementation (Figure 10c). The cementation of sandy dolomite is obvious, which is mainly manifested in the distribution of spun calcite and pyrite crystal aggregates. Dolomite sandstone is mainly cemented by calcite or iron dolomite. Pyrite crystals and calcite aggregates are distributed in granular and plaque shapes. Feldspar detritus sandstone is in point-line contact, and the cementation type is mostly pore-contact cementation. The calcite crystals are squeezed between the clastic particles, resulting in the cements (Figure 10d). The pyrite crystal aggregates are filled in the intergranular pores in the form of round particles. Most of the calcites are strongly replaced by feldspar fragments and some of the feldspar fragments are replaced by calcite along the cleavage joints (Figure 10f). Feldspar detritus sandstone is mainly

represented by the replacement of granular plagioclase by clay minerals. Part of the mudstone clastics is chloritized, and the secondary growth of feldspar and quartz can be seen.

4.4. Pore Structure

4.4.1. Reservoir Spaces

The pore space of the shale oil reservoir comprises the organic pore, inorganic pore and microfracture (Figure 11). Organic pores mainly consist of primary and dissolved organic pores. Inorganic pores can be divided into primary pores and secondary pores, including the intergranular pore of minerals, intragranular pore of minerals, intercrystalline pore and intracrystalline pore (Table 3).

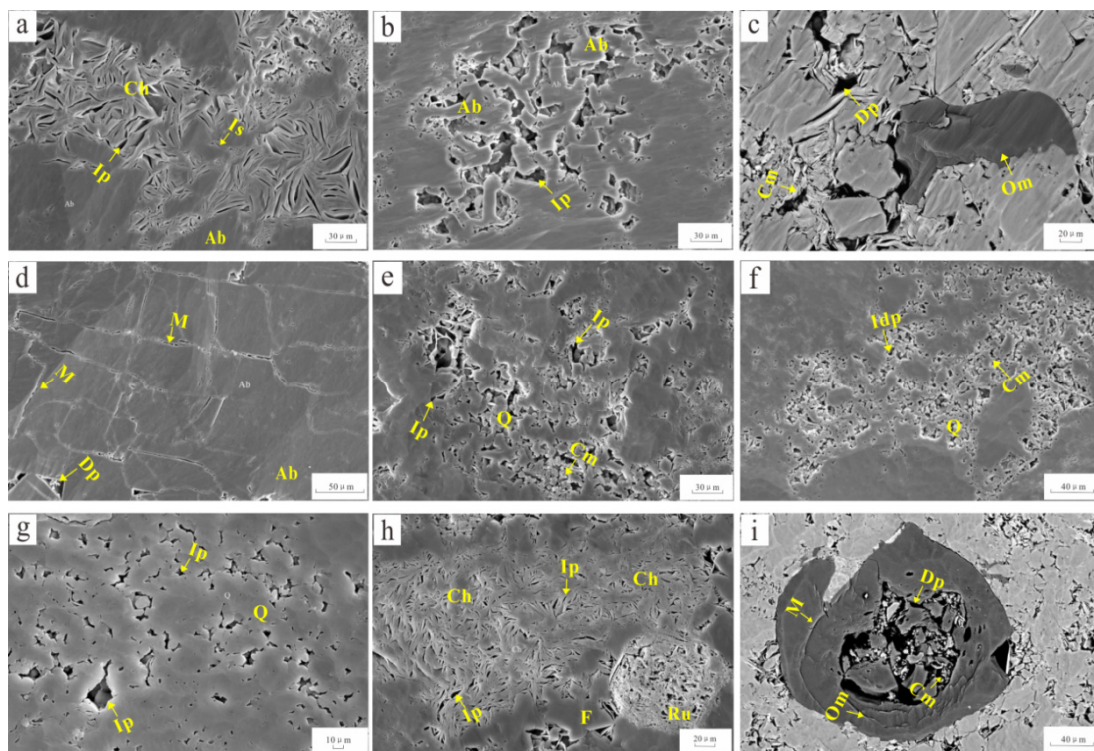


Figure 11. SEM images of the shale samples of the Lucaogou Formation in Jimsar Sag. (a). Dolomite sandstone. J10022, 3469.7 m. Albite is partially chloritized and some interlayer seam (Is) and Intercrystalline pores (Ip) can be seen in the thin section; (b). Dolomite sandstone. J10022, 3469.9 m. Albite is dissolved to form intragranular pores (Ip), filled with a small amount of clay minerals; (c). Dolomite sandstone. J10022, 3457.9 m. The dissolved pores (Dp) are filled with the scattered organic matter (Om) and clay minerals (Cm); (d). Dolomite siltstone. J10016, 3317.5 m. The network of micro-cracks and a small amount of dissolved pores (Dp) are formed by the dissolution of albite (Ab); (e). Feldspar detritus sandstone. J10016, 3296.4 m. The intragranular pores (Ip) are formed by the dissolution of lithic, which are partially filled by clay minerals (Cm) and authigenic quartz (Q); (f). Feldspar detritus sandstone. J10016, 3452.2 m. The intragranular dissolved pores (Idp) are filled with authigenic quartz crystals and a small amount of clay minerals (Cm); (g). Sandy dolomite. J10016, 3317.1 m. The intergranular pores (Ip) are filled with the authigenic quartz crystallites and a small amount of clay minerals, and the intercrystalline pores develop in the quartz; (h). Feldspar detritus sandstone. J10016, 3296.4 m. The chlorite intercrystalline pores (Ip) developed in the feldspar and some rutile aggregates (Rn) can be seen in the thin section; (i). Feldspar detritus sandstone. J10016, 3296.4 m. The detrital minerals are broken by the organic matter. Organic matter pores and microcracks (M) developed between organic matter (Om) and detrital minerals.

Table 3. Reservoir space type of the Lucaogou Formation in Jimsar Sag.

| Cause Type | Pore Type | Cause Mechanism | Feature | Pore Size/ μm |
|-----------------|------------------------------------|--|---|--------------------------|
| Primary pores | Residual intergranular pores | Mostly residual pores between particles | Mostly triangular or polygonal generally distributed in isolation poor connectivity | 30–80 |
| | Intercrystalline pores | | | |
| Secondary pores | Intergranular dissolution pores | Partial dissolution of particles such as feldspar or cuttings and partial dissolution of interstitials form interstitial dissolution pores | Irregular, scattered, small pores and fine throat | >0.01 |
| | Matrix dissolution pores | | | |
| | Intercrystalline dissolution pores | | | |

The primary pores are mainly remaining intergranular pores with clear pore boundaries, and the particles are not filled by miscellaneous bases and cements. They are one kind of the important storage spaces in the reservoir. The secondary pores are mainly produced by the dissolution, which are generally developed in most of the lithology in the reservoir. They are the most important pore type in the reservoir. A microfracture can be occasionally observed in the study area, but they are relatively undeveloped. The intragranular pores, intergranular pores and intercrystalline pores are observed by the scanning electron microscopy, while the degree of development of primary pores and organic pores are relatively low.

4.4.2. Pore Throat Distribution

The high-pressure mercury intrusion experiment technology can directly and quantitatively describe the distribution of effective pore throat volume and reveal information such as pore throat size, connectivity and sorting [38–40]. The capillary pressure curve has low discharge pressure and high mercury removal efficiency, indicating the pore throat structure and the sorting are good. According to the capillary pressure curve of the shale oil in the Lucaogou Formation, the mercury curve can be divided into weak platform shape, low slope linear shape, high slope linear shape and upward convex shape, which represent different types of pore throat combinations.

High-pressure mercury intrusion curves and pore size distribution curves of 12 samples are shown in Figure 12, with detailed information shown in Table 4. The results reveal varied intrusion curves and wide pore size distributions in these samples, indicating strong microscopic heterogeneity in the pore throat structure. The mercury intrusion curve of feldspar detritus sandstone is a weak platform. The pore throat radius mainly ranges from 0.10 to 0.63 μm , and the displacement pressure is scattered with a wider range from 1.27 to 2.55 MPa with an average of 1.91 MPa. The maximum pore throat radius is between 0.288 and 0.580 μm with an average of 0.430 μm . The maximum mercury saturation mainly ranges from 80.7 to 97.2% with an average of 88.08%. The displacement pressure of high slope linear samples is usually small and the pore throat radius mainly ranges from 0.1 to 0.4 μm . The pore throat connection relationship is complex. The displacement pressure mainly ranges from 0.63 to 2.55 MPa with an average of 1.24 MPa. The maximum pore throat radius mainly ranges from 0.288 to 1.167 μm . The maximum mercury inlet saturation ranges from 72.8 to 89.8% with an average of 81.125%. The low slope linear sample has a high displacement pressure with low mercury saturation, but the distribution range of pore throat is small. The lithology is mainly lithic feldspar sandstone and sandstone dolomite. The pore throats radii are between 0.016 and 0.063 μm . The displacement pressure mainly ranges from 10.23 to 20.45 MPa with an average of 12.785 MPa. The maximum pore throat radii are between 0.036 and 0.072 μm with an average of 0.063 μm .

The maximum mercury saturation mainly ranges from 75.5 to 83.6% with an average of 79.375%. The convex sample has a high drainage pressure and a low mercury removal efficiency. The pore throat radius is usually less than 0.03 μm . They usually develop in dolomitic mudstone, which makes it difficult to distinguish the pore and throat. It is usually composed of clay intercrystalline pores and other intercrystalline pores. In general, the Lucaogou shale oil reservoir has high displacement pressure, low mercury removal efficiency, large variation of pore throat distribution and poor pore throat connectivity.

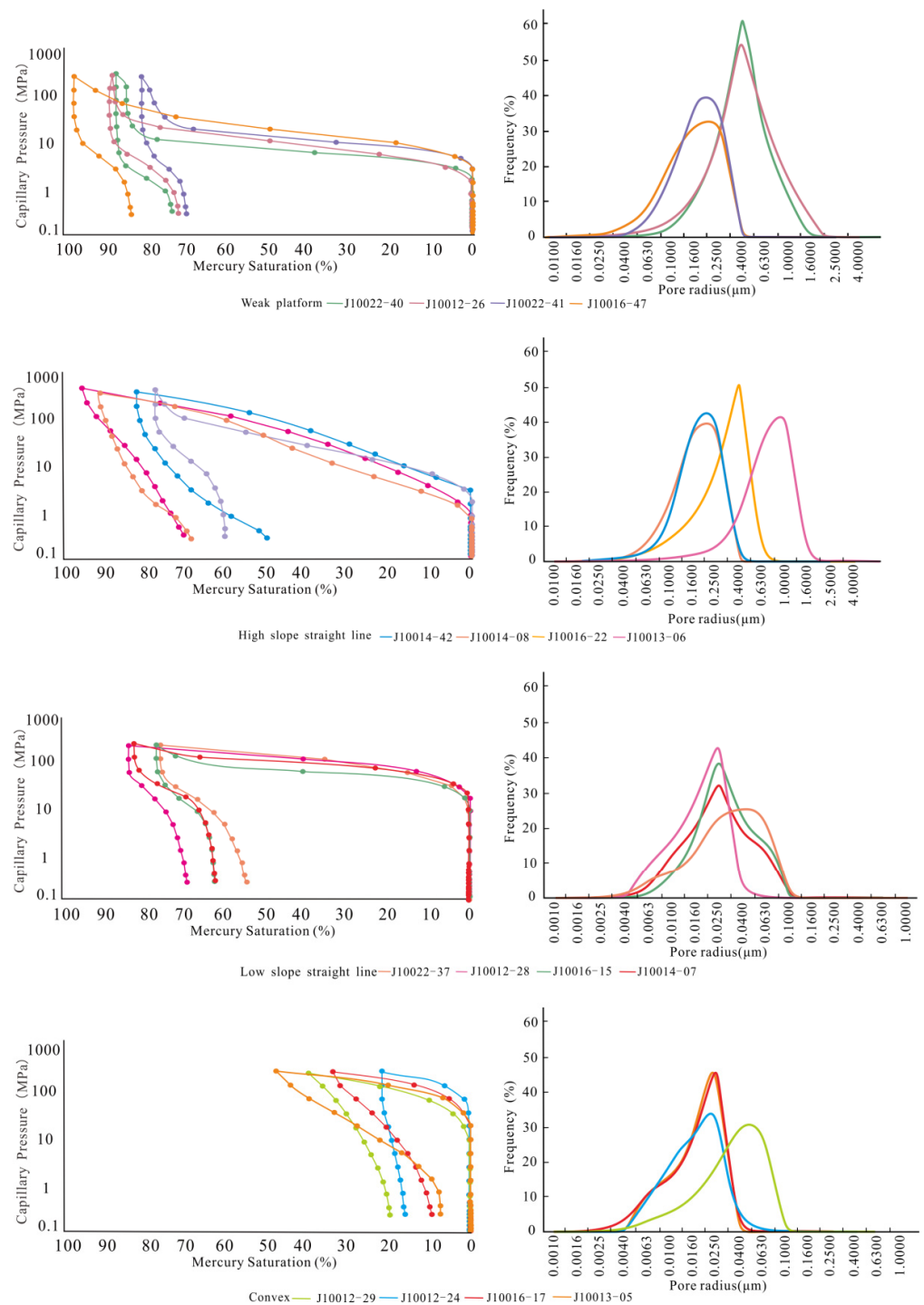


Figure 12. The curve shape of high-pressure mercury intrusion, and the distribution characteristics of pore size distribution.

Table 4. Testing data of high-pressure mercury injection of the Lucaogou Formation in Jimsar Sag.

| Curve Shape | Sample | Porosity/% | Permeability/mD | Median Radius/ μm | Discharge Pressure/Mpa | Maximum Pore Throat Radius/ μm | Maximum Mercury Saturation/% |
|----------------------------|-----------|------------|-----------------|------------------------------|------------------------|---|------------------------------|
| Weak platform | J10012-26 | 10.700 | 0.030 | 0.140 | 1.270 | 0.580 | 87.600 |
| | J10022-40 | 14.000 | 0.040 | 0.220 | 1.270 | 0.580 | 86.800 |
| | J10022-41 | 11.600 | 0.010 | 0.100 | 2.550 | 0.288 | 80.700 |
| | J10016-47 | 10.900 | 0.010 | 0.070 | 2.550 | 0.288 | 97.200 |
| High slope linear straight | J10014-42 | 1.200 | 0.020 | 0.009 | 2.550 | 0.288 | 76.700 |
| | J10014-08 | 4.200 | 0.480 | 0.028 | 0.630 | 1.167 | 85.200 |
| | J10016-22 | 7.600 | 0.020 | 0.039 | 1.270 | 0.580 | 72.800 |
| | J10013-06 | 3.500 | 0.020 | 0.023 | 0.630 | 1.167 | 89.800 |
| Low slope linear straight | J10022-37 | 4.600 | 0.010 | 0.007 | 10.230 | 0.072 | 75.500 |
| | J10012-28 | 3.700 | 0.010 | 0.007 | 20.450 | 0.036 | 83.600 |
| | J10016-15 | 10.700 | 0.010 | 0.014 | 10.230 | 0.072 | 76.700 |
| | J10014-07 | 7.300 | 0.030 | 0.011 | 10.230 | 0.072 | 81.700 |
| Upward convex | J10012-29 | 1.300 | 0.130 | — | 10.230 | 0.072 | 38.100 |
| | J10012-24 | 0.800 | 0.020 | — | 20.450 | 0.036 | 20.700 |
| | J10016-17 | 1.700 | 0.200 | — | 20.450 | 0.036 | 32.700 |
| | J10013-05 | 0.500 | 0.010 | — | 20.450 | 0.036 | 46.200 |

4.4.3. Pore Throat Structures

The sample specific surface area can be calculated by the BET equation. The pore diameter distribution, pore volume and the average aperture can be calculated by the BJH method [41,42]. According to the nitrogen adsorption experiment data of each sample, the isotherm adsorption/desorption curve and pore size distribution diagram are shown in Figure 13, with detailed pore structure parameters shown in Table 5. The specific surface area of the shale oil of the Lucaogou Formation in Jimsar Sag is scattered with a wide range from 0.61 to 4.23 m^2/g . The pore volume mainly ranges from 2.14 to 14.89 mm^3/g , and the average pore diameter is scattered with a range from 8.34 to 45.38 nm.

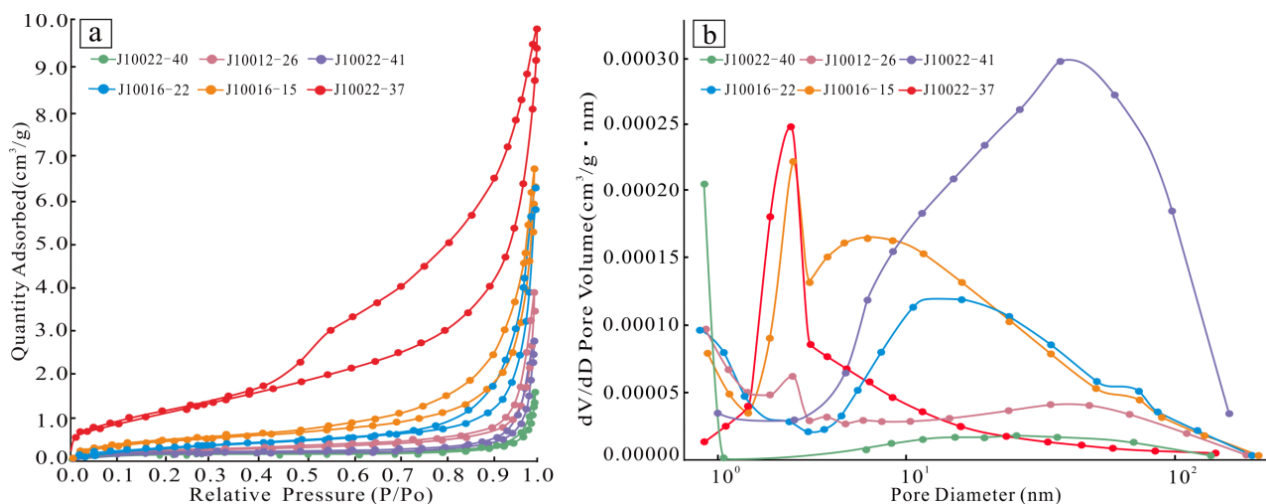


Figure 13. Adsorption–desorption isotherm (a) and pore size distribution of shale oil samples (b) of the Lucaogou Formation in Jimsar Sag.

Table 5. The pore throat parameters of nitrogen adsorption of the Lucaogou Formation in Jimsar Sag.

| Sample | Specific Surface Area/m ² /g | Pore Volume/mm ³ /g | Average Pore Diameter/nm | Peak Pore Diameter Distribution/nm |
|-----------|---|--------------------------------|--------------------------|------------------------------------|
| J10012-26 | 0.83 | 5.51 | 29.40 | 3.64 |
| J10022-40 | 0.61 | 2.14 | 29.52 | 27.42 |
| J10022-41 | 0.71 | 3.70 | 45.38 | 40.02 |
| J10022-37 | 40.23 | 14.89 | 8.34 | 3.75 |
| J10016-15 | 1.60 | 9.49 | 20.48 | 3.88 |
| J10016-22 | 1.12 | 8.89 | 26.81 | 12.86 |

The adsorption isotherm of most samples basically coincides with the desorption isotherm. When the relative pressure is close to 1, the amount of nitrogen adsorption rises sharply and the hysteresis loop has the characteristics of the H3 type hysteresis loop, which indicates that slit-like pores are developed in shale [43]. The hysteresis loops of some samples are relatively large, indicating that the pores of various sizes are relatively developed and the pore connectivity is better. The corresponding pore diameters are mainly distributed with a range from 1 to 40 nm. The corresponding relationship between the average pore diameter and the specific surface area of most samples is basically consistent. The peak pore diameter of shale is from a few nanometers to tens of nanometers, most of which are less than 50 nanometers, indicating that small pores have a greater contribution to the pore volume and specific surface area.

5. Discussion

5.1. Classification of Different Pore Throat Structures

According to the analysis of sedimentary diagenesis on pore type and the mechanism of pore structure development, the pore throat structure can be divided into four types in combination with the characteristics of different pore pressure curve morphologies and aperture distribution frequency curves: (i) larger pore medium-fine throats, (ii) medium pore medium throats; (iii) medium pore fine throats, (iv) fine pore fine throats.

Based on the mercury intrusion data and thin slice data (Figure 14), the pore throat radius of type I mainly ranges from 0.10 to 0.63 μm with a good sorting. The pore types are mainly intergranular dissolution pores and residual intergranular pores, which have the characteristics of large-pore fine throats with a relatively good pore throat connection relationship. The pore throat radius of type II mainly ranges from 0.1 to 0.4 μm . The intergranular dissolution pores are developed, and the pore throat connection relationship is relatively good. The pore throat radius of type III is mainly distributed in 0.016–0.063 μm . The pore types are mainly the intergranular dissolution pores and intercrystalline pores with a complex pore throat connection relationship. The pore throat radius of type IV is mostly less than 0.03 μm with a poor sorting. The clay intercrystalline pores and other intercrystalline pores together constitute this type of reservoir space. The results of mercury intrusion experiments and pore structure types show that the pore structures of different lithology and physical properties are different in characteristics. It is feasible to classify the pore structure in combination with pore type and pore throat radius distribution frequency.

5.2. Main Controlling Factors of the Pore Throat Structure

Tectonic movement controls the supply direction of provenance, the distribution and evolution of sedimentary facies. The sedimentation controls the material basis and spatial distribution of reservoir formation, and the thickness and type of sediments also lay the foundation for the type and intensity of diagenesis. While the diagenesis is the key factor that promotes changes in the pore structure of the reservoir.

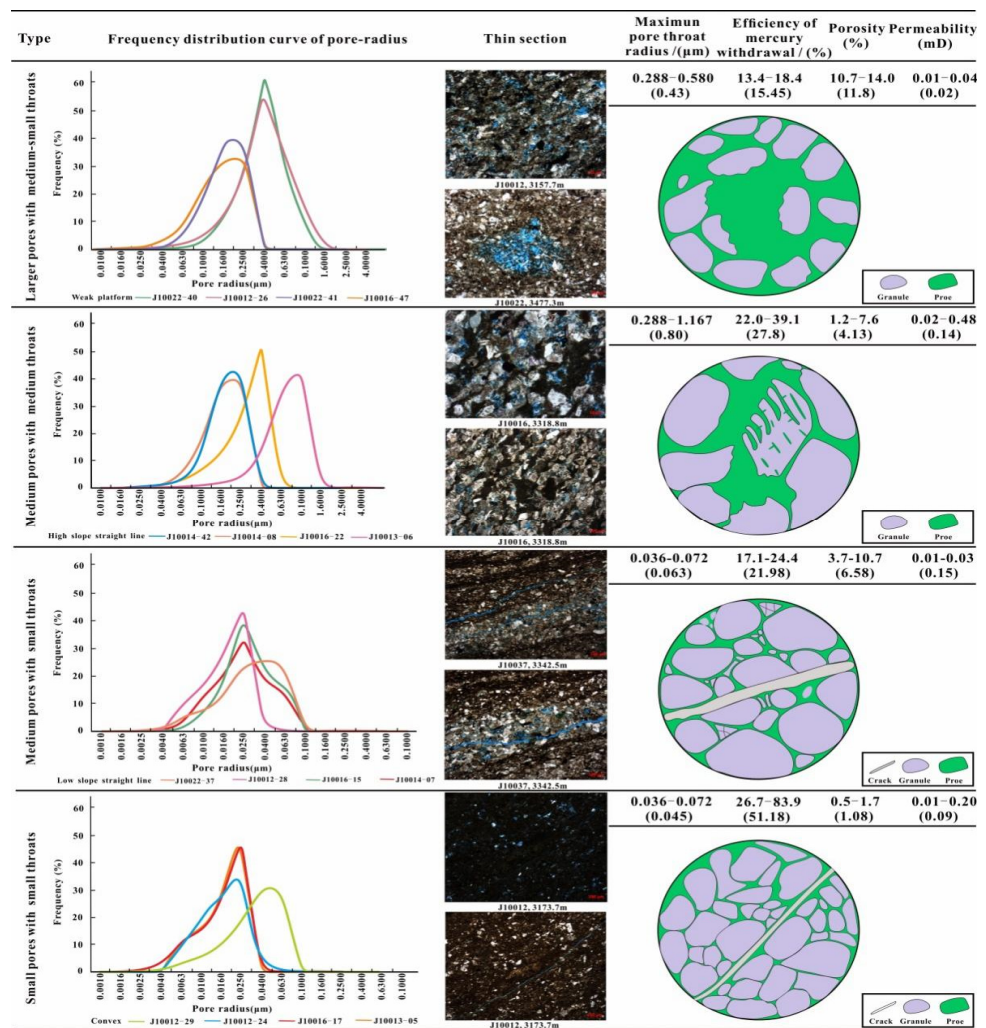


Figure 14. Characteristics of the pore throat structures of the Lucaogou Formation in Jimsar Sag.

5.2.1. Tectonism

The Lucaogou Formation in the Jimsar Sag is located in a slope structure and has experienced multiple periods of tectonic movement such as Hercynian, Indosinian, Yanshan and Himalayas, but the internal tectonic activity in the sag is relatively weak. The Lucaogou Formation has not experienced a strong tectonic uplift and did not expose the surface in the supergene stage, which is conducive to the preservation of dissolved pores [31]. The Jimsar Sag was affected by strong tectonic subsidence and formed a large-scale lacustrine sedimentary environment under an extensional background in the early Middle Permian. Volcanic activities were frequent and a large amount of volcanic ash material provided a sufficient material basis for the Jimsar Sag in this period. The lake basin water has a high degree of salinity because of the strong evaporation. The Ca^{2+} and Mg^{2+} released by the volcanic material are conducive to the precipitation of carbonate components and provide carbonate components for mixed deposition. Different degrees of dissolution occurred under the action of alternating acid-base fluid dissolution and transformation, which greatly improved the physical properties of the reservoir. The difference of the pore throat structure is due to the various lithologically unstable components and contents.

5.2.2. Sedimentation

The Lucaogou Formation in Jimsar Sag mainly develops lacustrine and delta deposits [27,44]. Different sedimentary facies have different rock types and reservoir properties, which are the basis for various diagenetic processes and the evolution of later

secondary pores. Sedimentary facies can directly affect the formation and distribution of different reservoirs [45], leading to the differences in microscopic pore throat structures. As shown in Figure 1b, the delta front facies mainly developed in the marginal zone of the depression, dominated by the feldspar detritus sandstone. Most of the pores mainly consist of the primary intergranular pores and remaining intergranular pores. Many unstable minerals are corroded by acidic fluids to form dissolved pores, which have good physical properties, relatively large pores and good pore throat connectivity. The large-pore medium-fine throat and medium-pore medium throat are the main pore throat structure types, which are the most favorable reservoirs. The central area of the sag is transformed into a shallow lake facies, and the overall physical properties become worse. The capillary pressure curve shape gradually changes from weak platform shape and high slope linear shape to the low slope linear shape and upward convex shape (Figure 15). Intergranular dissolved pores of the dolomite sandstone and dolomite in shallow lakes are relatively developed in an alkaline environment. The main pore throat structure type is medium-pore fine throats. The physical conditions of the reservoir are improved by the dissolution of feldspar and dolomite, making the porosity and permeability of shallow lake facies second to the delta front facies. The argillaceous siltstone, silty mudstone and mudstone are developed in the semi-deep lake-deep lake facies. The porosity and permeability conditions are worse than those in the lacustrine and delta front facies. The capillary pressure curve is mainly a low slope linear shape and upward convex with a pore throat structure of fine-pore fine throats.

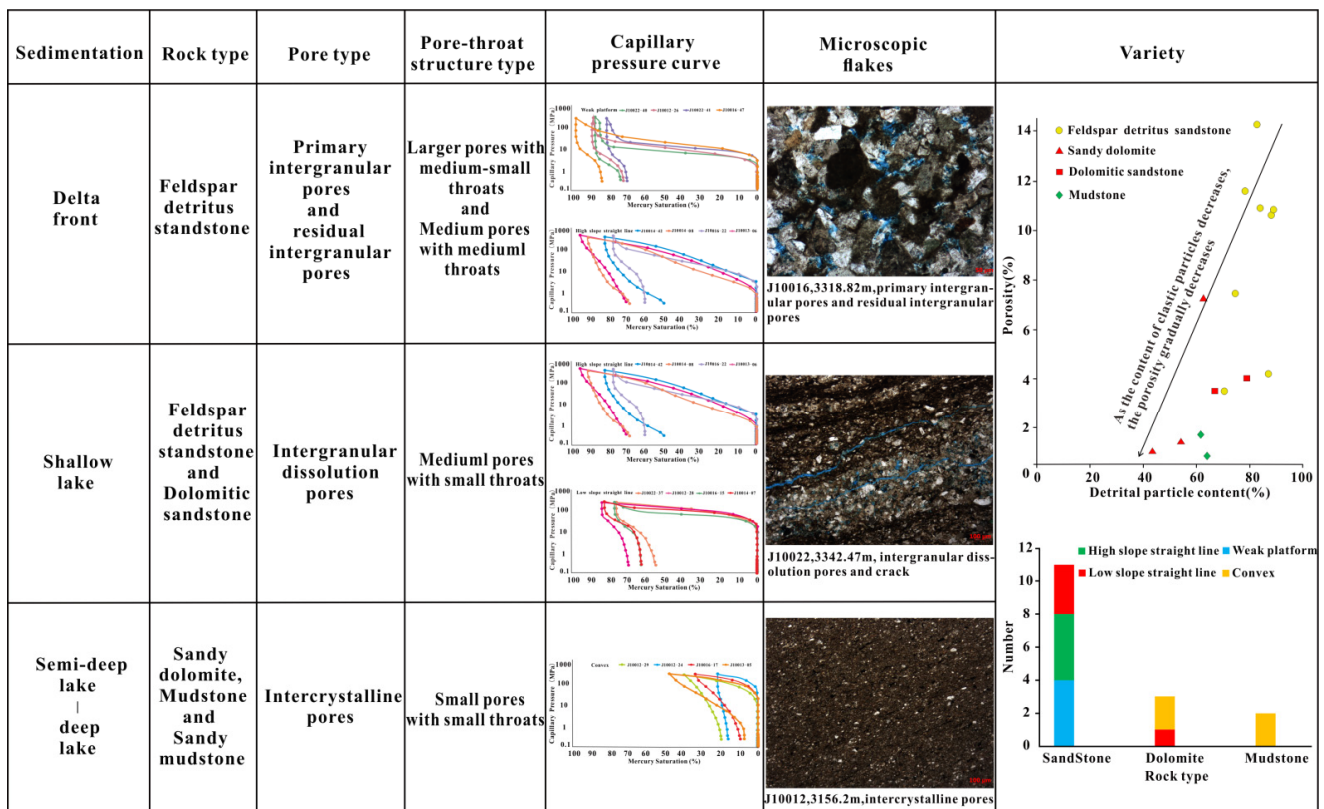


Figure 15. Distribution characteristics of pore throat structure in different sedimentary facies.

5.2.3. Diagenesis

The shale oil reservoir of the Lucaogou Formation in Jimsar Sag has undergone various types of diagenetic processes. The major destructive diagenetic processes in the Lucaogou Formation are the compaction and cementation, which together make the physical properties worse and the pore throat structure complex. The dissolution is the major constructive

diagenetic process, which can improve the reservoir quality [46]. In this paper, the porosity of dominant lithology of Lucaogou Formation in different diagenesis types is restored. The contribution of different diagenesis stages to the increase or decrease in reservoir porosity is quantitatively evaluated. Finally, the influence of different diagenesis on reservoir pores is clarified and the evolution law of different pore structures is discussed [47].

The shale oil reservoir of the Lucaogou Formation in Jimsar Sag has complex lithology and varied mineral composition. Ten rock samples are selected (the content of terrigenous detrital component is more than 80%) in the research. The rock sorting coefficient, cement content, primary intergranular porosity, cement face rate, dissolution pore face rate and the total face rate are counted (Table 6). Finally, the original porosity of sandstone is calculated by the empirical formula [48].

Table 6. The reduction in porosity parameters of the Lucaogou Formation in Jimsar Sag.

| Lithology | Sorting Coefficient | Cement Content | Primary Intergranular Porosity/% | Cement Face Rate/% | Dissolution Pore Face Rate/% | Porosity/% | Total Face Rate/% |
|-----------------------------|---------------------|----------------|----------------------------------|--------------------|------------------------------|------------|-------------------|
| Detrital feldspar sandstone | 4.20 | 6.24 | 4.32 | 13.68 | 13.86 | 11.97 | 17.26 |
| Dolomitic sandstone | 2.60 | 5.37 | 9.36 | 16.85 | 15.24 | 9.98 | 18.23 |

Original porosity calculation formula:

$$\Phi_0 = 20.91 + 22.90/S_0 \quad (1)$$

S_0 is the Trask sorting coefficient, $S_0 = P_{25}/P_{75}$, obtained in the cumulative curve of particle size probability. P_{25} is the particle size corresponding to the content of 25% on the cumulative particle size curve, and P_{75} is the particle size corresponding to the content of 75% on the cumulative particle size curve.

Compaction is the fundamental reason for the deterioration of the physical properties of the reservoir. The calculation formula for the porosity of the sandstone after compaction is as follows [49]:

$$\Phi_1 = [(\Phi_{pm} + \Phi_{ca}) \times \Phi_p / \Phi_t] + C_t \quad (2)$$

$$\Phi_L = \Phi_0 - \Phi_1 \quad (3)$$

$$F_L = (\Phi_L / \Phi_0) \times 100\% \quad (4)$$

Φ_0 —original porosity/%; Φ_1 —sandstone porosity after compaction/%; Φ_L —compaction loss porosity/%; Φ_p —physical property analysis porosity/%; Φ_t —total face rate/%; Φ_{pm} —primary intergranular porosity/%; Φ_{ca} —cement face rate/%; C_t —cement content/%; F_L —compacted porosity loss rate/%.

After compaction, cementation and metasomatic diagenesis, the residual porosity is the post-consolidation porosity. The calculation formula is as follows:

$$\Phi_2 = \Phi_{ps} / \Phi_t \times \Phi_p \quad (5)$$

$$\Phi_S = \Phi_0 - \Phi_1 - \Phi_2 \quad (6)$$

$$F_S = (\Phi_S / \Phi_0) \times 100\% \quad (7)$$

Φ_2 —sandstone porosity after cementation/%; Φ_S —cementation loss porosity/%; Φ_{ps} —intergranular porosity/%; F_S —cemented porosity loss rate/%.

Dissolution can improve the physical properties of the reservoir and improve the storage performance. The porosity after dissolution is equivalent to the sum of the porosity after cementation and the porosity increased by dissolution [50]. The calculation formula is as follows:

$$\Phi_3 = \Phi_{pd} / \Phi_t \times \Phi_p \quad (8)$$

$$\Phi_D = \Phi_3 + \Phi_2 \tag{9}$$

$$F_D = (\Phi_D / \Phi_0) \times 100\% \tag{10}$$

Φ_3 —increased porosity by dissolution/%; Φ_D —porosity after dissolution/%; Φ_{pd} —dissolution pore area ratio/%; F_D —porosity enhancement by dissolution/%.

From the above calculations, it can be seen that the feldspar detritus sandstone of the Lucaogou Formation in Jimsar Sag has medium-good sorting with a sorting coefficient of 4.20, and the calculated initial porosity is about 26.36%. The sorting of dolomitic sandstone is relatively poor with a sorting coefficient of 2.60, and the calculated initial porosity is about 29.72%. The compacted porosity loss rates of feldspar detritus sandstone mainly range from 15.26 to 38.51% with an average of 28.98%. The cemented porosity loss rate mainly ranges from 10.86 to 24.35% with an average of 17.60%. The compacted porosity loss rate of dolomite sandstone mainly ranges from 14.85 to 34.85% with an average of 33.65%. The cemented porosity loss rate mainly ranges from 12.59 to 35.86% with an average of 16.55%. In general, the compaction is the main cause of pore loss, and the dissolution is the main cause of porosity increase. The porosity increase rate mainly ranges from 5.34 to 7.96% with an average of 5.38%. The pore throat structure of shale oil reservoirs in the Lucaogou Formation in Jimsar Sag is mainly controlled by compaction, dissolution and cementation. The storage properties are improved to a certain extent by the alternating action of acid-base fluids. This conclusion is consistent with the results observed under the microscope.

Based on the above analyses, sedimentation, diagenesis, and tectonism worked together to give rise to pore throat structure differences. The early carbonate mineral dissolution of favorable sedimentary facies, the dissolution of a large number of feldspars, tuffaceous minerals and a small amount of carbonate cements by organic acids are the key factors to improve the pore throat structure of the reservoir, which have formed a good larger-pore medium-fine throats and medium-pore medium throats (Figure 16).

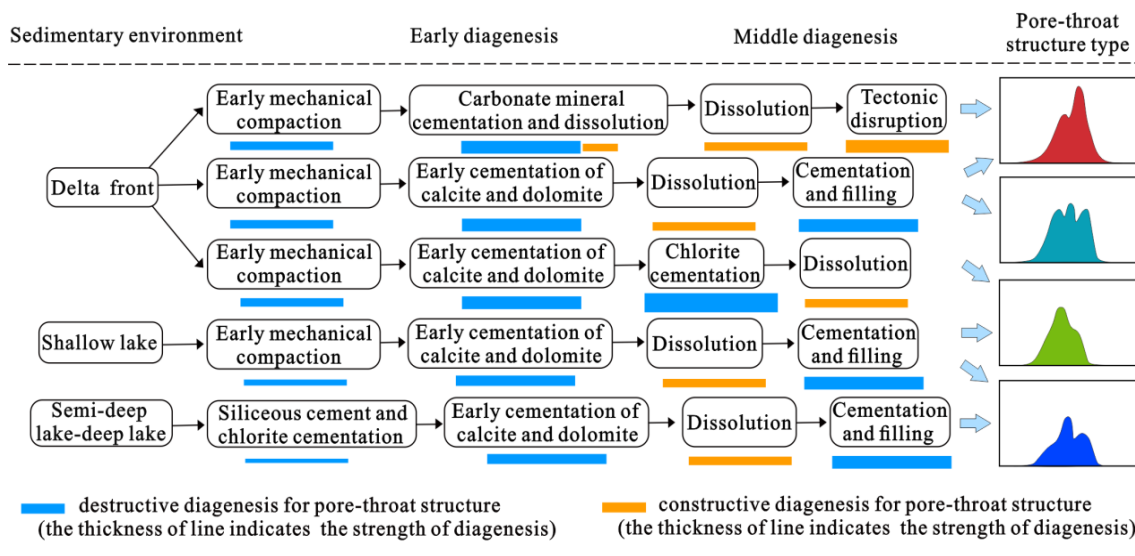


Figure 16. The evolution of pore throat structures under the control of sedimentary environments, diagenetic processes and tectonism of the Lucaogou Formation in Jimsar Sag.

5.3. Genetic Evolution Models of Different Pore Throat Structures

The sedimentary facies of shale oil reservoirs of the Lucaogou Formation in Jimsar Sag are different, which have different diagenetic assemblage types. According to the basic characteristics of the reservoir and the relationship of different diagenesis, the diagenetic assemblage types of the study area are divided into three diagenetic assemblage types: (1) weak compaction–weak carbonate cementation–strong dissolution. (2) Medium compaction–strong calcite and dolomite cementation–weak dissolution.

(3) Strong compaction–strong calcite cementation–weak dissolution. The different diagenetic assemblage type has differences in the pore throat structure. The type 1 and type 2 of diagenetic assemblage types mainly develop large-pore middle throats and medium-pore middle throats. The third type of diagenetic assemblage types mainly develops the medium-pore fine throats and the fine-pore fine throats.

Combined with the previous studies of the buried thermal evolution history and the diagenetic evolution sequence of shale oil reservoirs of the Lucaogou Formation in Jimsar Sag [51], the genetic evolution models of different pore throat structures of the Lucaogou Formation are comprehensively discussed by the characteristics of a thin section under microscope and the diagenetic assemblage types.

5.3.1. Genetic Evolution Model of Large Pore Medium Throats and Medium Pore Medium Throat Reservoirs

For the large-pore medium throat and medium-pore medium throat reservoirs, the early compaction of the reservoir is relatively weak, and the mineral particles are in point-line contact. The chlorite film fills the pores in the form of lining edges because of the alkaline characteristics of formation water during the early diagenetic deposition period, which increases the ability of the reservoir to resist compaction. Early calcite was produced in the form of a continuous crystal base, which further cemented the primary intergranular pores. It is the compaction and cementation that cause the pores to decrease with a range from 3.91 to 9.19%. At the same time, the diagenetic environment changed from alkaline to weakly acidic because of the early hydrocarbon generation of early diagenesis. The organic acids inhibit the cementation of early calcite and at the same time produce a small amount of feldspar and carbonate minerals to dissolve. A large amount of organic acids entered the reservoir to cause large-scale dissolution of feldspar, clastics and partial cements during the middle diagenetic deposition period. The dissolution pores formed by the dissolution of organic acids mainly ranges from 1.59 to 2.37%. At this time, part of the alkaline feldspar and acid corrosion product kaolinite reacted to form the illite and illite/smectite minerals. As a result of the large amount of acidic fluid consumed, the pore water medium gradually changes from an acidic to alkaline diagenesis environment and switches to the alkaline diagenesis environment again. The compaction and cementation further occurred at the same time. The dolomite was cemented in the late stage, and the iron dolomite replaced calcite. The final reservoir porosity is 10% (Figure 17).

5.3.2. Genetic Evolution Model of Medium Pore Fine Throat and Fine Pore Fine Throat Reservoirs

A diagenetic law of strong compaction–strong cementation–weak dissolution was revealed in this study area, which directly controls the evolution of porosity [32]. For the medium-pore fine throat and the fine-pore fine throat reservoirs, the main diagenetic assemblage type is strong compaction–strong calcite cementation–weak dissolution. The early compaction of the reservoir is strong, and the volcanic clastics have certain directional arrangement characteristics. At the same time, the rock debris undergoes the plastic deformation and the pseudo hybridization blocks the pore throats, resulting in a significant decrease in the primary intergranular pores [52]. The porosity drops rapidly, and the amount of pore reduction because of the compaction mainly ranges from 4.50 to 11.45%. The primary intergranular pores were further cemented by the early calcite. At this time, the cementation pore reduction was about 3.49%. The diagenetic environment changed from alkaline to weakly acidic by the influence of early hydrocarbon generation of early diagenesis. Organic acids inhibited the early calcite cementation. A part of the feldspar and carbonate minerals were dissolved by the organic acids. The dissolution of feldspar, clastics and some cements occurred during the middle diagenetic sedimentation period, resulting in some secondary pores. The dissolution pores were increased with a range from 1.41 to 2.10%. The illite and illite/smectite minerals are the product of the acidic dissolution, which filled in the pores of the grains, occupying the pores and blocking the throat. As a result of the large amount of acidic fluid consumed, the pore water medium

gradually changes from an acidic to alkaline diagenesis environment and switches to the alkaline diagenesis environment again. The compaction and cementation occurred again. The cementation of late carbonate minerals and clay minerals resulted in a final reservoir with a porosity of 8% (Figure 18).

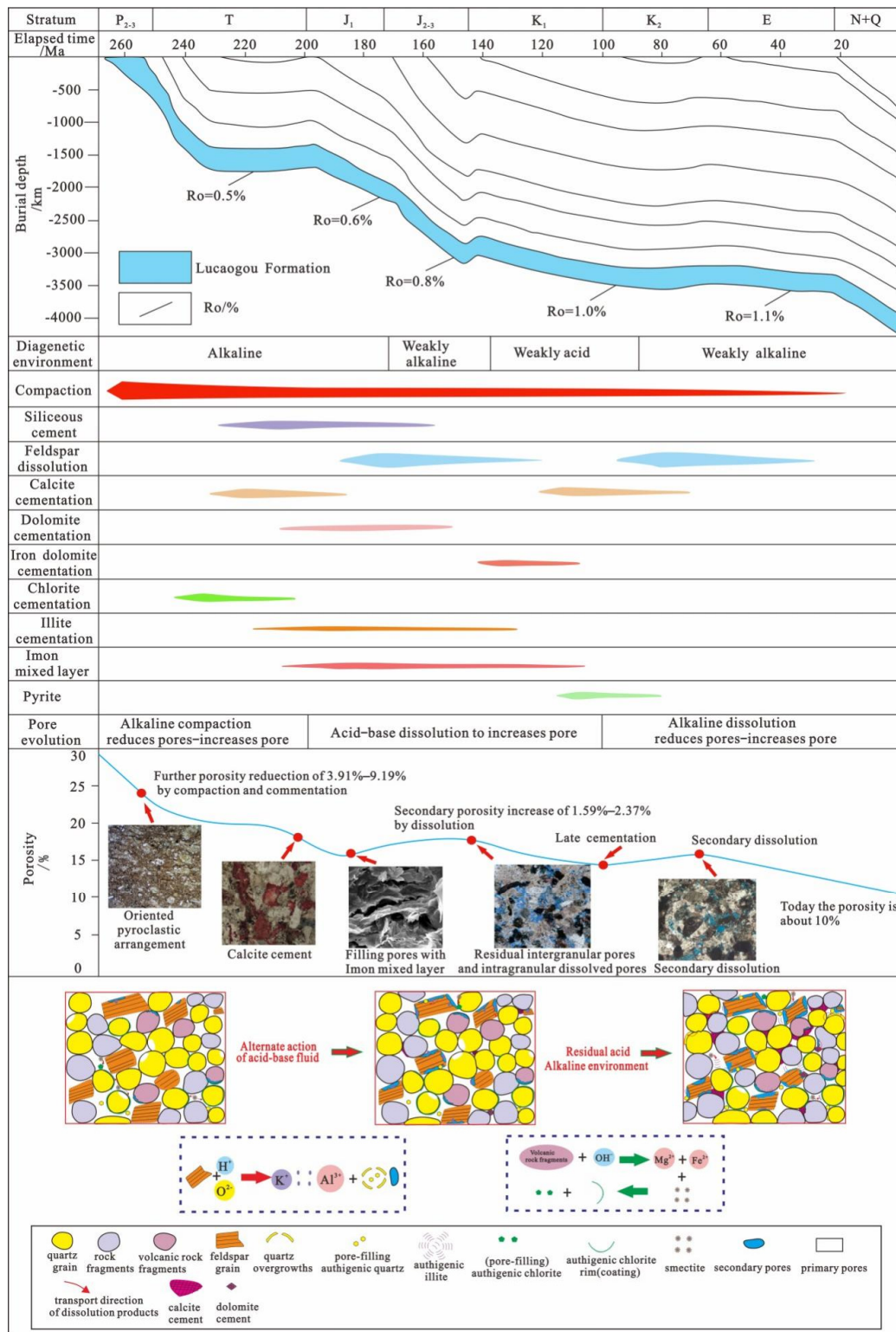


Figure 17. Genetic evolution model of large pore medium-fine throats and medium pore medium throats.

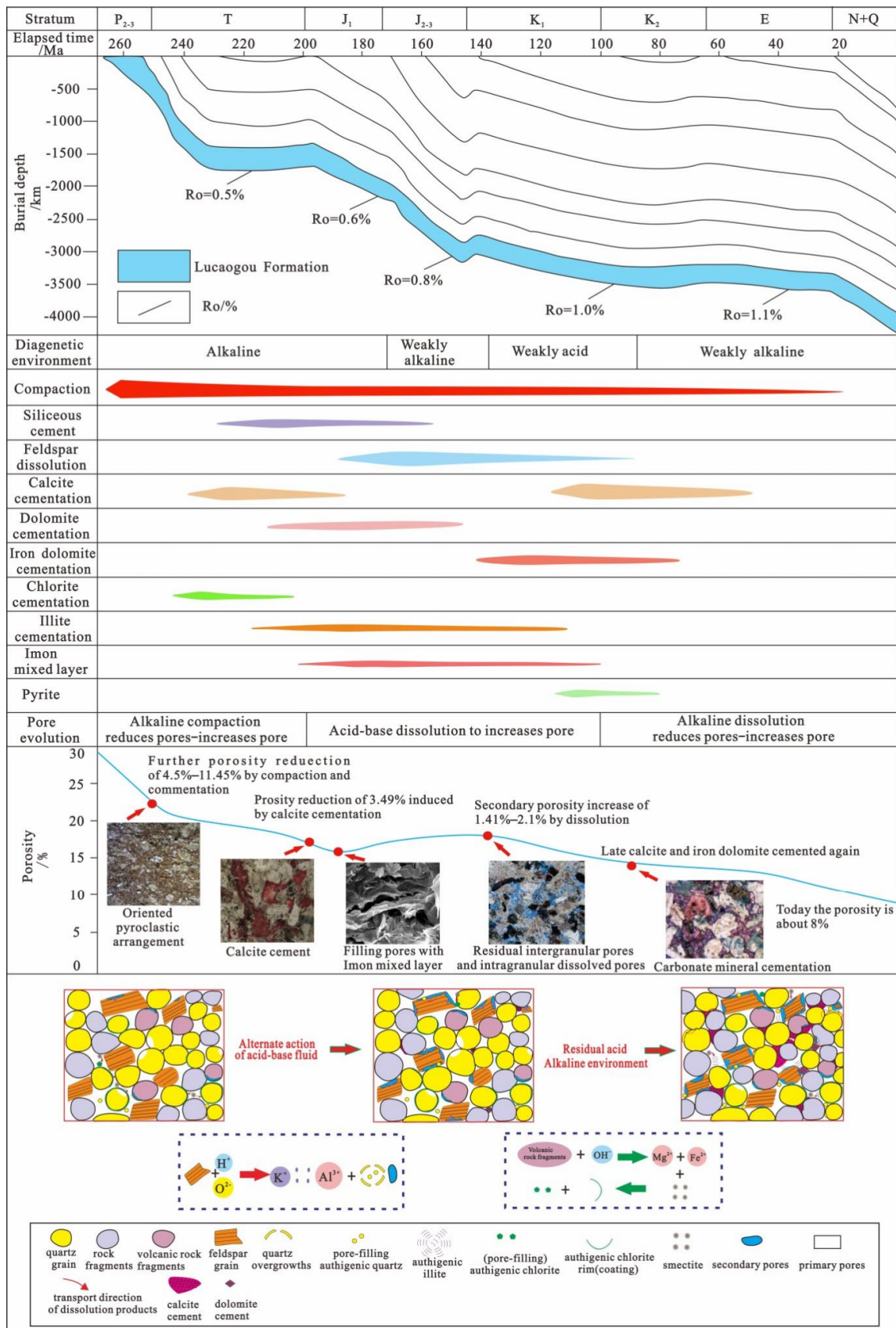


Figure 18. Genetic evolution model of medium pore fine throats and fine pore fine throats.

6. Conclusions

The shale oil reservoir of the Lucaogou Formation in Jimsar Sag is characterized by complex lithology and diverse mineral components. The different lithologies have great differences in physical properties. The reservoir spaces mainly consist of residual intergranular pores, dissolved pores, intercrystalline pores and fractures.

The pore throat structure of shale oil reservoirs of the Lucaogou Formation in Jimsar Sag can be divided into four types. Type I is the large pore medium-fine throats with good sorting. The pore throat radius of the type I mainly ranges from 0.10 to 0.63 μm . Type II is the medium pore medium throats with good sorting. The pore throat radius of the type II is concentrated in the range from 0.1 to 0.4 μm . Type III is the medium pore fine throats with poor sorting and a complex connection relationship. The pore throat radius of type III is mainly distributed in 0.016–0.063 μm . Type IV is the fine pore fine throats with extremely poor sorting. The pore throat radius of the type IV is mostly less than 0.03 μm .

The main factors controlling the differences of pore throat structures are tectonic movement, sedimentary environment and diagenesis. The volcanic tectonic movement provides a sufficient material foundation for the Lucaogou Formation in Jimsar Sag. The lithologies of delta front facies consist of detrital feldspar sandstone, dolomite sandstone and dolomite, which are characterized by large-pore medium-fine throats and medium-pore medium throats. The lithologies of shallow lake-semi-deep lake facies consist of dolomite sandstone, argillaceous siltstone and mudstone. The pore throat structures of these lithologies mainly consist of the medium-pore fine throats and fine-pore fine throats with poor physical properties. Early compaction and cementation are the main factors leading to the reduction in pores and the deterioration of physical properties. The early carbonate mineral dissolution of favorable sedimentary facies, the dissolution of a large number of feldspars, tuffaceous minerals and a small amount of carbonate cements by organic acids are the key factors to improve the pore throat structure of the reservoir.

The genetic evolution models of pore throat structures of shale oil reservoirs of the Lucaogou Formation in Jimsar Sag are divided into two types. One is the genetic evolution models of large pore medium-fine throat and medium pore medium throat reservoirs. The early compaction of the reservoir is relatively weak, and some chlorite films increase the ability of the reservoir to resist compaction. The large-scale dissolution among feldspar, clastics and partial cements occur due to the effect of organic acids. The current porosity of the reservoir decreases up to 10% as a result of these processes. The other one is the genetic evolution models of medium pore fine throat and fine pore fine throat reservoirs. The early compaction of the reservoir is strong, resulting in a significant decrease in the primary intergranular pores. Then the primary intergranular pores were further cemented by the early calcite. A part of feldspar and carbonate minerals were dissolved by organic acids and some secondary pores were formed. The cementation of late carbonate minerals and clay minerals resulted in a final reservoir with a porosity of 8%.

Author Contributions: Conceptualization, X.T. and F.L.; methodology, L.L.; software, J.W.; validation, X.G., X.Z. and X.T.; formal analysis, F.L.; investigation, X.L.; resources, S.P.; data curation, Y.G. and Y.L.; writing—original draft preparation, X.Z.; writing—review and editing, X.Z.; visualization, X.G.; supervision, X.T.; project administration, X.T.; funding acquisition, X.G., L.L., N.J. and X.T. All authors have read and agreed to the published version of the manuscript.

Funding: This work is supported by the National Natural Science Foundation of China (Grant Numbers. 41902153, 42072140 and 42102133), Natural Science Foundation Project of Chongqing (Grant Numbers. cstc2021jcyj-msxmX0455 and cstc2020jcyj-msxmX0217), and Science and Technology Research Program of Chongqing Municipal Education Commission (Grant Numbers. KJQN201801522, KJQN202101544, KJZD-M202101502 and KJQN202001517).

Acknowledgments: We are grateful to the Research Institute of Petroleum Exploration and Development, PetroChina Xinjiang Oilfield, for permission to access their in-house database, providing background geologic data and permission to publish the results.

Conflicts of Interest: The authors declare no conflict of interest.

References

1. Breyer, J.A. *Shale Reservoirs: Giant Resources for the 21st Century*; AAPG Memoir; American Association of Petroleum Geologists: Tulsa, OK, USA, 2012; Volume 97, pp. 1–451.
2. Holditch, S.A. Unconventional oil and gas resource development-let's do it right. *J. Unconv. Oil Gas Resour.* **2013**, *1*–2, 2–8. [[CrossRef](#)]
3. Davies, R.J.; Almond, S.; Ward, R.S.; Jackson, R.B.; Adams, C.; Worrall, F.; Herringshaw, L.G.; Gluyas, J.G.; Whitehead, M.A. Oil and gas wells and their integrity: Implications for shale and unconventional resource exploitation. *Mar. Pet. Geol.* **2014**, *56*, 239–254. [[CrossRef](#)]
4. Huo, Z.; Hao, S.; Liu, B.; Zhang, J.; Ding, J.; Tang, X.; Li, C.; Yu, X. Geochemical characteristics and hydrocarbon expulsion of source rocks in the first member of the Qingshankou Formation in the Qijia-Gulong Sag, Songliao Basin, Northeast China: Evaluation of shale oil resource potential. *Energy Sci. Eng.* **2020**, *8*, 1450–1467. [[CrossRef](#)]
5. Zou, C.; Yang, Z.; Cui, J.; Zhu, R.; Hou, L.; Tao, S.; Yuan, X.; Wu, S.; Lin, S.; Wang, L.; et al. Formation mechanism, geological characteristics and development strategy of nonmarine shale oil in China. *Pet. Explor. Dev.* **2013**, *40*, 14–26. [[CrossRef](#)]
6. Lu, S.; Huang, W.; Chen, F.; Wang, M.; Xue, H.; Wang, W.; Cai, X. Classification and evaluation criteria of shale oil and gas resources: Discussion and application. *Pet. Explor. Dev.* **2012**, *39*, 249–256. [[CrossRef](#)]
7. Yang, Z.; Zou, C.; Wu, S.; Lin, S.; Pan, S.; Niu, X.; Men, G.; Tang, Z.; Li, G.; Zhao, J.; et al. Formation, distribution and resource potential of the “sweet areas (sections)” of continental shale oil in China. *Mar. Pet. Geol.* **2019**, *102*, 48–60.
8. Zhang, J.; Lin, L.; Li, Y.; Tang, X.; Zhu, L.; Xing, Y.; Jiang, S.; Jing, T.; Yang, S. Classification and evaluation of shale oil. *Earth Sci. Front.* **2012**, *19*, 322–331.
9. Song, J.; Littke, R.; Weniger, P.; Ostertag-Henning, C.; Nelskamp, S. Shale oil potential and thermal maturity of the Lower Toarcian Posidonia Shale in NW Europe. *Int. J. Coal Geol.* **2015**, *150–151*, 127–153. [[CrossRef](#)]
10. Wang, C.; Kuang, L.; Gao, G. Difference in hydrocarbon generation potential of the shaly source rocks in Jimusar, Permian Lucaogou Formation. *Acta Sedimentol. Sinica* **2014**, *32*, 385–390.
11. Nelson, P.H. Pore-throat sizes in sandstones, tight sandstones, and shales. *AAPG Bull.* **2009**, *93*, 329–340. [[CrossRef](#)]
12. Feng, Q.; Xu, S.; Xing, X.; Zhang, W.; Wang, S. Advances and challenges in shale oil development: A critical review. *Adv. Geo-Energy Res.* **2020**, *4*, 406–418. [[CrossRef](#)]
13. Wood, D.A. Techniques used to calculate shale fractal dimensions involve uncertainties and imprecisions that require more careful consideration. *Adv. Geo-Energy Res.* **2021**, *5*, 153–165. [[CrossRef](#)]
14. Wang, Y.; Gao, Y.; Fang, Z. Pore throat structure and classification of Paleogene tight reservoirs in Jiyang depression, Bohai Bay Basin, China. *Pet. Explor. Dev.* **2021**, *48*, 266–278. [[CrossRef](#)]
15. Jin, J.; Yang, Z.; Erxiding, Y.; Li, L.; Liu, M. Nanopore Characteristics and Oil-Bearing Properties of Tight Oil Reservoirs in Jimsar Sag, Junggar Basin. *Earth Sci.* **2018**, *43*, 1594–1601.
16. Li, W.; Mu, L.; Zhao, L.; Li, J.; Wang, S.; Fan, Z.; Shao, D.; Li, C.; Shan, F.; Zhao, W.; et al. Pore-throat structure characteristics and its impact on the porosity and permeability relationship of Carboniferous carbonate reservoirs in eastern edge of Pre-Caspian Basin. *Pet. Explor. Dev.* **2020**, *47*, 1027–1041. [[CrossRef](#)]
17. Zou, C.; Zhu, R.K.; Bai, B.; Yang, Z.; Wu, S.; Su, L.; Dong, D.; Li, X. First discovery of nano-pore throat in oil and gas reservoir in China and its scientific value. *Acta Petrol. Sin.* **2011**, *27*, 1857–1864.
18. Ren, X.; Li, A.; Wang, Y.; Wu, S.; Wang, G. Pore structure of tight sandstone reservoir and its influence on percolation: Taking the Chang 8 reservoir in Maling oilfield in Ordos Basin as an example. *Oil Gas Geol.* **2015**, *36*, 774–779.
19. Yang, F.; Ning, Z.; Wang, Q.; Kong, D.; Peng, K.; Xiao, L. Fractal characteristics of nanopore in shales. *Nat. Gas Geosci.* **2014**, *25*, 618–623.
20. Tian, W.; Liu, H.; He, S.; Wang, J.; Xie, L. Characterization of microscopic pore structure of tight oil reservoirs in Lucaogou Formation, Jimusaer Sag. *Pet. Geol. Recovery Effic.* **2019**, *26*, 25–30.
21. Liu, Y.; Dong, X.; Yan, L.; Chen, F.; Gao, Y.; Chen, Z. Quantitative Characterization of Pore Structure of the Lucaogou Formation in Jimsar Sag. *Xinjiang Pet. Geol.* **2019**, *40*, 284–289.
22. Liu, L.; Min, L.; Sun, Z.; Pei, L.; Gu, H. Pore structure and percolation characteristics in shale oil reservoir of Jiyang Depression. *Pet. Geol. Recovery Effic.* **2021**, *28*, 107–114.
23. Clarkson, C.R.; Solano, N.; Bustin, R.M.; Bustin, A.M.; Chalmers, G.R.; He, L.; Melnichenko, Y.B.; Radliński, A.P.; Blach, T. Pore structure characterization of North American shale gas reservoirs using USANS/SANS, gas adsorption, and mercury intrusion. *Fuel* **2013**, *103*, 606–616. [[CrossRef](#)]
24. He, L.; Zhao, L.; Li, J.; Ma, J.; Liu, R.; Wang, S.; Zhao, W. Complex relationship between porosity and permeability of carbonate reservoirs and its controlling factors: A case of platform facies in Precaspian Basin. *Pet. Explor. Dev.* **2014**, *41*, 206–214. [[CrossRef](#)]
25. Qin, R.; LI, X.; Liu, C.; Mao, Z. Influential factors of pore structure and quantitative evaluation of reservoir parameters in carbonate reservoirs. *Earth Sci. Front.* **2015**, *22*, 251–259.
26. Wang, Q.; Zhao, S.; Wei, Q.; Xiao, L.; Yang, Y.; Guo, Y.; Niu, M. Marine carbonate reservoir characteristics of the Middle Ordovician Majiagou Formation in Ordos Basin. *J. Palaeogeogr.* **2012**, *14*, 229–242.
27. Liu, H.; Yang, Y.; Wang, F.; Deng, X.; Liu, Y.; Nan, J.; Wang, J.; Zhang, H. Micro pore and throat characteristics and origin of tight sandstone reservoirs: A case study of the Triassic Chang 6 and Chang 8 members in Longdong area, Ordos Basin, NW China. *Pet. Explor. Dev.* **2018**, *45*, 239–250. [[CrossRef](#)]

28. Ma, K.; Liu, Y.; Hou, J.; Huang, S.; Yan, L.; Chen, F.; Yang, W. Mixed sedimentary model of salinized Lake in Lucaogou Formation of Permian in Jimusar Depression. *Acta Pet. Sin.* **2017**, *38*, 636–648.
29. Shao, Y.; Yang, Y.; Wan, M.; Qiu, L.; Cao, Y.; Yang, S. Sedimentary characteristics and sedimentary facies evolution of Permian Lucaogou Formation in Jimusar Sag. *Xinjiang Pet. Geol.* **2015**, *36*, 635–642.
30. Zhang, Y.; Ma, S.; Gao, Y.; Li, Y.; Zhang, J.; Wang, L.; Sun, Y.; Xu, F.; Li, H. Depositional facies analysis on tight reservoir of the Lucaogou Formation in Jimusar Sag, Junggar Basin. *Acta Sedimentol. Sin.* **2017**, *35*, 358–370.
31. Fang, S.; Song, Y.; Xu, H.; Fang, R.; Liu, L.; Xiu, X. Relationship between tectonic evolution and petroleum system formation—taking the Jimusar sag of eastern Junggar basin as an example. *Pet. Geol. Exp.* **2007**, *29*, 149–153.
32. Qu, C. *Characteristics and Depositional Environment of Organic-Rich Mixed Sedimentary Rocks in Permian Lucaogou Formation, Jimusar Sag*; China University of Petroleum: Beijing, China, 2017.
33. Yang, Y.; Liu, Y.; Jiang, Y.; Yang, Z.; Zhou, D.; Jiao, X.; Zhou, P.; Li, X.; Jin, M. Geochemistry of the dolomitic rocks from the Permian Lucaogou Formation in the Jimusar depression, Junggar Basin, Xinjiang. *Sediment. Geol. Tethyan Geol.* **2019**, *39*, 85–93.
34. Ma, K.; Liu, Y.; Hou, J.; Huang, S.; Yan, L.; Chen, F.; Yang, W. Densification Mechanism of Tight Reservoirs from Mixed Sedimentation in Saline Lacustrine Environment: A Case Study of Permian Lucaogou Formation, Jimusar sag. *Xinjiang Pet. Geol.* **2019**, *40*, 253–259.
35. Li, S. *Study on the Mixed Rock Microenvironment of the Lucaogou Formation in Jimusar Depression*; School of Geosciences Yangtze University: Jinzhou, China, 2020.
36. Bai, B.; Zhu, R.; Wu, S.; Wu, S.; Yang, W.; Gelb, J.; Gu, A.; Zhang, X.; Su, L. Multi-scale method of Nano(Micro)-CT study on microscopic pore structure of tight sandstone of Yanchang formation, Ordos Basin. *Pet. Explor. Dev.* **2013**, *40*, 329–333. [[CrossRef](#)]
37. Zhou, P. *Tight Oil Reservoir Characteristics and Reservoir Evaluation of Permian Lucaogou Formation in Jimusar Depression, Xinjiang*; Northwest University: Xi'an, China, 2014.
38. Wang, J.; Xiao, D.; Lu, S.; Kong, X.; Fang, Q. Classification evaluation of shale oil reservoir physical properties in Lucaogou formation, jimsar sag. *J. China Univ. Min. Technol.* **2020**, *49*, 173–183.
39. Wang, R.; Hu, Z.; Sun, C.; Liu, Z.; Zhang, C.; Gao, B.; Du, W.; Zhao, J.; Tang, W. Comparative analysis of shale reservoir characteristics in the Wufeng-Longmaxi (O3w-S11) and Niutitang (Є1n) Formations: A case study of the Wells JY1 and TX1 in southeastern Sichuan Basin and its periphery, SW China. *Interpretation* **2018**, *6*, SN31–SN45. [[CrossRef](#)]
40. Wang, R.; Hu, Z.; Dong, L.; Gao, B.; Sun, C.; Yang, T.; Wang, G.; Yin, S. Advancement and trends of shale gas reservoir characterization and evaluation. *Oil Gas Geol.* **2021**, *42*, 54–65.
41. Brunauer, S.; Emmett, P.; Teller, E. Adsorption of gases in multimolecular layers. *J. Am. Chem. Soc.* **1938**, *60*, 309–319. [[CrossRef](#)]
42. Barrett, E.P.; Joyner, L.G.; Halenda, P.P. The determination of pore volume and area distributions in porous substances. I. Computations from nitrogen isotherms. *J. Am. Chem. Soc.* **1951**, *73*, 373–380. [[CrossRef](#)]
43. Sing, K.S.W. Reporting physisorption data for gas/solid systems with special reference to the determination of surface area and porosity (Recommendations 1984). *Pure Appl. Chem.* **1985**, *57*, 603–619. [[CrossRef](#)]
44. Cao, Y.; Zhu, N.; Zhang, S.; Xi, K.; Xue, X. Diagenesis and Reserving Space Characteristics of Tight Oil Reservoirs of Permian Lucaogou Formation in Jimusar Sag of Junggar Basin, China. *J. Earth Sci. Environ.* **2019**, *41*, 253–266.
45. Zhang, Z.; Tian, J.; Han, C.; Zhang, W.; Deng, S.; Sun, G. Reservoir characteristics and main controlling factors of the Lucaogou Formation in Jimusar Sag, Junggar Basin. *Lithol. Reserv.* **2021**, *33*, 116–126.
46. Dai, C.; Zheng, R.; Zhu, R.; Li, F.; Gao, Z.; Bai, B. Reservoir characteristics of the Xujiahe Formation in central-west Sichuan analogus foreland basin. *Nat. Gas Geosci.* **2011**, *27*, 47–55.
47. Yu, C. Pore structure characteristics and formation mechanism of Chang 8 member tight sandstone reservoir in Fuxian area. *Unconv. Oil Gas* **2021**, *8*, 15–21.
48. Bear, D.C.; Weyl, P.K. Influence of texture on porosity and permeability of unconsolidated sand. *AAPG Bull.* **1973**, *57*, 349–369.
49. Scherer, M. Parameters influencing porosity in sandstones: A model for sandstone porosity prediction. *AAPG Bull.* **1987**, *71*, 485–491. [[CrossRef](#)]
50. Wang, R.; Chen, M. Quantitative analysis of porosity evolution during the reservoir sedimentation diagenesis-taking the Yan 25 and Zhuang 40 areas in the Ordos Basin as examples. *Acta Geol. Sin.* **2007**, *81*, 1432–1437.
51. Wang, J.; Zhou, L.; Liu, J.; Zhang, X.; Zhang, F.; Zhang, B. Acid-base alternation diagenesis and its influence on shale reservoirs in the Permian Lucaogou Formation, Jimusar Sag, Junggar Basin, NW China. *Pet. Explor. Dev.* **2020**, *47*, 898–912. [[CrossRef](#)]
52. Wang, M.; Tang, H.; Liu, S.; Zhao, F.; Li, L.; Lu, H.; Wang, Y.; Zhang, L. Formation mechanism of differential sandstone densification modes and its impact on reservoir quality: A case study of Upper Paleozoic Permian in eastern part of Sulige gasfield, Ordos basin. *J. China Univ. Min. Technol.* **2017**, *46*, 1228–1246.